B-T-3294

The Hardness, Adhesion, and Wear Resistance of Coatings Developed for Cobalt-base Alloys

B.V. Cockeram and W. L. Wilson

USDOE contract No. DE-AC11-98PN38206

BETTIS ATOMIC POWER LABORATORY WEST MIFFLIN, PENNSYLVANIA 15122-0079

Operated for the U.S. Department of Energy
by Bechtel Bettis, Inc.

DISCLAIMER

The Hardness, Adhesion, and Wear Resistance of Coatings Developed for Cobalt-base Alloys

B.V. Cockeram* and W.L. Wilson

Bechtel-Bettis Atomic Power Laboratory, P.O. Box 79, West Mifflin, PA 15122-0079.

*Corresponding Author. Tel.: 412-476-5647; fax: 412-476-5151.
E-mail address: cockeram@bettis.gov (B.V. Cockeram)

Abstract

One potential approach for reducing the level of nuclear plant radiation exposure that results from activated cobalt wear debris is the use of a wear resistant coating. However, large differences in stiffness between a coating/substrate can result in high interfacial stresses that produce coating deadhesion when a coated substrate is subjected to high stress wear contact. Scratch adhesion and indentation tests have been used to identify four promising coating processes [1,2]: (1) the use of a thin Cr-nitride coating with a hard and less-stiff interlayer, (2) the use of a thick, multilayered Cr-nitride coating with graded layers , (3) use of the duplex approach, or nitriding to harden the material subsurface followed by application of a multilayered Cr-nitride coating, and (4) application of nitriding alone. The processing, characterization, and adhesion of these coating systems are discussed. The wear resistance and performance has been evaluated using laboratory pin-on-disc, 4-ball, and high stress rolling contact tests. Based on the results of these tests, the best coating candidate from the high-stress rolling contact wear test was the thin duplex coating, which consists of ion nitriding followed deposition of a thin Cr-nitride coating, while the thin Cr-nitride coating exhibited the best results in the 4-ball wear test.

1. Introduction

Cobalt-base alloys possess outstanding wear and corrosion resistance, but the nuclear activation of cobalt wear debris to Co^{60} results in high radiation levels in nuclear plant applications [3,4]. The costs resulting from nuclear plant contamination with Co^{60} debris could be reduced either by covering the cobalt-base alloy with a wear-resistant coating or substitution with a low cobalt alloy. Since the unique combination of wear and mechanical properties observed in cobalt-base alloys are rarely duplicated in cobalt-free systems, the use of a wear resistant coating involves less risk. Potential wear through or failure of the coating would only expose the wear resistant cobalt-base material.

Most cobalt-base alloys are significantly less stiff than wear resistant coatings. The use of a wear-resistant coating that has a higher stiffness or hardness than the base material typically

results in poor performance in high stress wear applications [5,6]. High stress wear contact results in high interfacial stresses between a stiff coating and a softer substrate, which typically leads to coating deadhesion. Catastrophic coating deadhesion produces large pieces of hard, abrasive coating debris and typically results in a high wear rate, which is the major risk associated with coating application. The approaches taken to develop coatings for cobalt-base alloys in this work were intended to produce an adherent coating and minimize differences in modulus/hardness between the wear resistant coating and base material [1,2], see Table 2. The adhesion properties of the coatings were evaluated using scratch adhesion testing, nano-scratch testing and nano-indentation testing. The most viable candidates were ultimately identified from the results of 4-ball, pin-on-disc, and high stress rolling-contact wear tests.

2. Base Materials and Procedures

2.1. Materials and Scratch Adhesion Tests

Nominal compositions for the two different cobalt-base alloys used in this work (Haynes 25 and Stellite 3) and a precipitation-hardening stainless steel (17-4 PH aged to the H1100 condition) are summarized in Table 1. Scratch adhesion testing was performed using a spherical indentor at constant load with visual examinations used to define the critical load. Nano-scratch adhesion testing was performed at MTS-Nano Instruments, Knoxville, TN using a sapphire sphere (130 μm diameter) or a cube corner (100 μm) indentor by increasing the load from 0 to 500 milli-Newtons or 0 to 30 milli-Newtons, respectively [1,8,9]. The critical load was identified by a large change in coefficient of friction or penetration depth during the nano-scratch test. Vickers or Knoop hardness was measured using a 10g load. Nano-indentation testing was performed using a Berkovich diamond indentor in the continuous stiffness mode [8]. The modulus or hardness values shown in Table 2 were determined at a nano-indentation depth less than 1/10 of the coating thickness. Nano-indentation hardness versus depth profiles typically exhibited a peak with no apparent plateau, which indicates that substrate deformation was influencing the hardness measurement [8].

2.2. 4-ball wear test

The procedure for the 4-ball wear testing that was performed at Falex Corporation, Sugar Grove, IL, has been reported previously [1,7]. Six test pieces are used in the 4-ball wear test: (1) one Haynes 25 cup (4.57 cm outer diameter, 2.15 cm inner diameter, 1.71 cm thick with a 0.66 cm radius for the raceway), (2) three Stellite 3 intermediate balls (1.27 cm diameter) that ride in the cup race within a 17-4 PH separator (4.28 cm diameter X 0.70 cm thick with three equally spaced holes 1.31 cm in diameter), and (3) one Haynes 25 drive ball (1.27 cm diameter) in point-contact with the intermediate balls for rotation and load application. The 6.21 kg load applied to the drive ball results in 2.42 GPa Hertzian contact stresses on the ball surfaces. The drive ball is rotated at 1200 RPM in room-temperature (20-30°C) de-ionized water. The cup, drive ball, and intermediate balls were covered with three different coatings for the 4-ball wear test (Table 2): (1) thin, dual-layer Cr-N(ss)/Cr_2N coating, (2) ion nitriding, and (3) thin duplex coating. Two tests were performed for each of the coating candidates and two sets of uncoated coupons (drive and intermediate balls, separator, and cup) were tested as controls for a total of eight tests. Weight change and profilometry (Taylor/Hobson Taly-surf profilometer) measurements were used to characterize wear [1,2].

2.3. Pin-on-disc wear test

Pin-on-disc wear testing was performed at Advanced Coating Technology Group at Northwestern University (ACTG) in room temperature distilled water at a rotational sliding speed of 0.1 m/s for a maximum of 30 minutes [2]. Application of 6.804 kg load to the Stellite 3 pin (1.3 cm length X 0.63 cm diameter with a 0.47 cm radius on the tip) on the Haynes 25 disc (5.72 cm diameter X 0.76 cm thick) produces an initial estimated Hertzian contact stress of 345 MPa. Torque and friction was continuously monitored, and the test was terminated if these values became excessively high. Two types of coatings were applied to either the pin or disc surface (Table 2): (1) 2.5 μm thick, dual-layer Cr-N(ss)/Cr_2N coating, and (2) 9 μm thick layer of tungsten.

2.4. Rolling-contact wear test

A Rolling Contact (RC) test was performed on all coating candidates to evaluate the wear resistance at high stresses. Three Haynes 25 rollers (Figure 1a) are mounted on an axle at 120°

intervals in a floating cage. Two opposed and loaded 17-4 PH bushings (Figure 1b) are positioned concentric with a rotating shaft and three Haynes 25 rollers, which are located between the bushings. The outer diameter of the Haynes 25 rollers were coated and the 17-4 PH bushings were not coated. As the bottom bushing is rotated at 26.5 RPM, the three rollers travel around the flat surface of each bushing. The center point of each roller contact experiences pure rolling while the inner and outer portions of contact are required to slip a small amount as the roller is forced to traverse the circular path (rather than a straight line which is the normal path for the roller). The resultant motion is therefore a combination of rolling and sliding contact. For the 0.3175 cm thick rollers, the percent of sliding is linear from zero at the pitch circle to 10 percent at the extremities of contact. The actual sliding velocity at the 10-percent slip location at 26.5 RPMs of rolling (1.778 cm/s) is 0.0178 cm/s. The test rig is mounted to the head of a 25.4 cm x 38.1 cm pressurized autoclave (12.4 MPa) through which high purity water at 149°C is circulated at 6.3 to 18.9 X 10^{-5} m^3/sec. The spring load used for these tests was 24.36 kg (8.12 kg per roller) which resulted in an initial Hertzian contact stress of 345 MPa on the center-line of roller/bushing contact. The load spring was calibrated before each test to establish the deflection required to achieve the specified load at temperature. Pre-test and post-test specimen inspections included surface finish, bushing thickness, and weight change (±0.1 mg) measurements. Post-test wear surfaces were characterized by visual inspections, scanning electron microscopy (SEM), and metallography with diametrical sections used to characterize the cross-section of the wear surface.

3. Coating Design Approach

An elastic, plane strain model that quantifies the coating/substrate interfacial stresses produced under high stress wear applications has been reported [5,6]. Assuming similar coating and substrate displacements, Lamé equations were used to relate stresses and displacement gradients in the x (σ_x and ε_x) and y (σ_x and ε_x) direction:

$$\sigma_x = 2G\varepsilon_x + \lambda(\varepsilon_x + \varepsilon_y) = 2G(\partial u/\partial x) + \lambda((\partial u/\partial x) + (\partial v/\partial y)) \quad (1)$$

$$\sigma_y = 2G\varepsilon_y + \lambda(\varepsilon_x + \varepsilon_y) = 2G(\partial v/\partial y) + \lambda((\partial u/\partial x) + (\partial v/\partial y)) \quad (2)$$

$$\tau_{xy} = G\gamma = G((\partial u/\partial y) + (\partial v/\partial x)) \quad (3)$$

where $G = E / (2 (1 + \mu))$ and $\lambda = \mu E / ((1 + \mu)(1 - 2\mu))$ are the Lamé constants, E is Young's modulus, μ is Poisson's ratio, and τ_{xy} is the shear stress for either the coating or substrate. Assuming the deformation is occurring by plane strain elasticity, Equations (1), (2), and (3) are further differentiated to derive displacement functions for the coating and substrate [5,6]. These displacement functions are used to derive a stress distribution by substitution into the Lamé equations [5,6]. The coating/substrate interfacial stresses that result from high stress contact are predicted to be higher and tensile in nature when the coating has a much higher modulus than the base material. The level of tensile coating/substrate interfacial stresses can be reduced using two approaches [6]: (1) increased coating thickness, and (2) use of a transition interlayer that has a modulus that is in between the substrate and the wear coating.

The approach for designing wear coatings for cobalt-base alloys was to match the modulus/hardness of the substrate as close as possible through the use of interlayers and/or reduce interfacial stresses by use of thicker coatings. Processes were selected that produce a tightly bonded coating through the use of diffusion growth methods (ion nitriding or plasma carburizing) or reactive, high energy PVD methods. Four types of coatings were developed: (1) a thin dual-layer Cr-nitride coating with a hard and softer interlayer, (2) thick, multilayer coatings with softer inner layers, (3) ion nitriding or plasma carburizing to grow a thick, adherent layer, and (4) duplex approach of plasma nitriding to harden the subsurface and support a graded, multilayer coating.

4. Coating Characterization

A listing of the various coating / surface modification systems which were evaluated, along with the results of nano-indentation and scratch testing, is presented in Table 2.

4.1 Multilayer Zr-nitride coatings

A cathodic arc PVD process was used to deposit a dual-layer zirconium-nitride (ZrN) coating that consisted of a thick (≈ 7.5 μm) outer layer and a thin (≈ 1.5 μm) inner layer of ZrN (ICDD card # 02-0956) [1,2]. Although a higher critical load value is expected for thicker coatings [8-10],

conventional and nano-indentation scratch test values for the ZrN coating were comparable to results for the thinner TiN and Cr-N(ss)/Cr_2N coatings (see Table 2). Nano-indentation hardness values for the ZrN and TiN coatings are more than a factor of three higher than bare Haynes 25. This large difference in hardness between Haynes 25 and the ZrN or TiN coatings indicates that wear under high stress loading would likely result in high interfacial stresses and coating deadhesion [5,6].

4.2 Multilayer Cr-nitride coatings

A reactive (nitrogen atmosphere), unbalanced magnetron (UBM) sputtering process was used to produce chromium-nitride (Cr-N(ss)/Cr_2N) coatings consisting of an outer Cr_2N layer (ICCD Card #35-0803) and an inner layer of chromium-nitrogen solid solution (Cr-N(ss), chromium with a lattice parameter = 2.887 ± 0.005 Å versus 2.884 Å for pure chromium), see Table 2 [1,2]. Both thick (2.5 μm) and thin (1 μm) dual-layer coatings, as well as a thicker (10.4 μm) 4-layer coating, were produced. The layers for the thin two-layer Cr-N(ss)/Cr_2N coating with a 2:1 ratio of Cr-N(ss) to Cr_2N are difficult to resolve in Figure 2a, but XRD analysis confirmed the layer identification. A thicker dual-layer Cr-N(ss)/Cr_2N coating with a 3:2 ratio was deposited on pins and discs.

The individual layers of the four-layer Cr-N(ss)/Cr_2N coating (≈10 μm) with a 4 μm inner Cr-N(ss) layer / 1 μm layer of Cr_2N / 4 μm layer of Cr-N(ss) / 1 μm outer layer of Cr_2N are clearly resolved by the chromium and nitrogen maps shown in Figures 2b, 2c, and 2d. The scratch adhesion value for the thick four-layer Cr-N(ss)/Cr_2N coating in Table 2 was higher than the thinner Cr-N(ss)/Cr_2N coatings, as expected for a thicker coating. The excellent adherence and larger thickness of the four-layer Cr-N(ss)/Cr_2N coating resulted in no coating damage with the nano-scratch method. Conventional hardness values for the thick, four-layer Cr-N(ss)/Cr_2N coating were comparable to values for the thinner Cr-N(ss)/Cr_2N coatings (Table 2). However, the use of a nano-indentation method results in hardness/modulus values for the thick four-layer Cr-N(ss)/Cr_2N coating that are lower than the thin Cr-N(ss)/Cr_2N coatings and close to the Haynes 25 base material. At a nano-indentation depth of 1 μm, only the top two layers (1 μm outer layer of Cr_2N and 4 μm inner

layer of Cr-N(ss)) of the four-layer coating were probed, which resulted in nano-indentation hardness/modulus values that match the base material. Conventional and nano-indentation scratch values for the thin dual-layer Cr-N(ss)/Cr_2N coating were higher than values measured for the ZrN and TiN coatings. Less severe scratch damage was observed for the thin dual-layer Cr-N(ss)/Cr_2N coating than for the adhesion testing of the ZrN and TiN coatings, which indicates that the Cr-N(ss)/Cr_2N coatings are more adherent and damage resistant. The lower critical load value for the 2.5 μm thick Cr-N(ss)/Cr_2N coating with the 3:2 ratio indicates that the use of a lower Cr-N(ss) fraction in the multilayer design, which likely results in less matching of coating/substrate hardness, degrades coating adhesion.

4.3. Thick tungsten coating

Thick (9 μm) tungsten coatings were deposited by UBM on pins and discs, see Table 2. SEM and XRD analysis confirmed that the coating was primarily crystalline tungsten with trace element concentrations below the EDS detection limit. Adhesion values were not determined, but the hardness of the tungsten coating was slightly lower than the Cr-N(ss)/Cr_2N coatings.

4.4. Ion Nitriding and Plasma Carburizing

One attempt was made to plasma carburize Haynes 25 using a glow discharge method at 593°C for 48 hours. The thick, porous deposit of amorphous carbon and oxygen that resulted from this plasma carburizing method was fragile with poor adherence, see Table 2 [1,2].

Ion nitriding is a commercial process involving the ionization of nitrogen gas in a dense plasma and acceleration of ionized nitrogen into the substrate to increase the surface hardness and wear resistance by the inward diffusion of nitrogen [11,12]. Cobalt has a low solubility for nitrogen. Ion nitriding therefore results in the growth of an adherent nitride layer with a diffusion zone that is about 1/4 the nitride layer thickness [1,2,11], see Table 2 and Figure 3. The interference between the nitrogen K-energy line and cobalt L-energy gives the false appearance of high nitrogen in the Haynes 25 substrate (see WDS map in Figure 3b). The true nitrogen content in the diffusion zone was below the detection limit (<0.1%). Microprobe and XRD analysis has shown that the nitride

layer is a (Co,Cr,W,Ni,Fe)N compound with the CrN structure (ICDD card #11-0065). The metal content of the nitride compound is comparable to the base material. Ion nitriding of Stellite 3 (Figure 3d) results in the formation of a thinner two-phase layer consisting of a (Co,Cr,W,Ni,Fe)N compound with Cr-carbides. Stellite 3 consists of Cr-carbides and Co-base dendrites, and the features of this microstructure are translated into the layer formed by ion nitriding. The growth kinetics of the nitride layer are slow, and the low activation energy (10.7 kJ/(mol K)) indicates that either a grain boundary diffusion, surface diffusion, or gaseous diffusion mechanism dominates the ion nitriding process [1]. Deposition from the steel fixturing resulted in the formation of a layer of nodules ($\approx 1\mu$m diameter) that were rich in iron + carbon on the surface of ion nitrided coupons, see Figure 3e.

Ion nitriding produced a large increase in the surface roughness of the balls (R_a = 130 Å → R_a = 2800-5300 Å) and cup (R_a = 250-1300 Å → R_a = 2800-4100 Å). Thermal activation and surface bombardment resulting from the ion nitriding [12] and the influence of gas-phase or surface kinetics on the growth of the nitride layer likely increases the surface roughness [1]. Accurate measurement of nano-indentation scratch values was difficult from the rough ion nitrided surfaces. A critical load for the nano-scratch test was not detected at the maximum applied load, and only ductile smearing of the iron-rich surface nodules was observed in Figure 3e. The depth of nano-indentation was on the order of the iron-rich surface nodules (1 μm), which results in the measurement of a low hardness/modulus value. Conventional hardness measurements have shown that the nitride compound is a factor of two harder than Haynes 25 (see Table 2).

4.5. Duplex Coatings (Ion Nitriding + Cr-N(ss)/Cr_2N Coatings)

Duplex coatings were produced by using an UBM process to deposit two different Cr-N(ss)/Cr_2N coatings on ion nitrided substrates: (1) a thin (1 μm) dual layer coating with a Cr-N(ss):Cr_2N ratio of 2:1, and (2) a thicker (6 μm) two-layer coating with a ratio of 4:1. Coating deposition on the rough surface of the ion nitride layer with the surface layer of iron-rich nodules was somewhat difficult, but adherent deposits were produced with little change in surface roughness [1,2]. An alternative, low-pressure duplex coating was performed by ion nitriding in the sputter

coating chamber at a significantly lower total pressure, nitrogen pressure (6:1 ratio of nitrogen to argon) and shorter time (1 hour) than used for commercial ion nitriding followed by UBM deposition of a thin (0.7 μm) dual-layer Cr_2N / Cr-N(ss) coating with a 3:2 ratio [1].

The BSE images and nitrogen x-ray maps in Figure 4 show that the duplex coatings consist of dual-layer Cr-N(ss)/Cr_2N coatings deposited on a nitride layer. Interference between the L-energy cobalt line and nitrogen energy line gives the false appearance of high nitrogen in the Haynes 25 substrate, as observed with the ion nitrided substrates. The presence of Cr_2N (ICDD card # 35-0803), Cr-N(ss), and nitride layer (card #11-0065) was confirmed using XRD for all duplex coatings. Conventional hardness and scratch adhesion values for the duplex coatings were comparable to values reported for Cr-N(ss)/Cr_2N coatings deposited on bare Haynes 25 (Table 2). Coating damage was not produced at the maximum applied load for a nano-indentation scratch test, which indicates that these coatings are adherent. Nano-indentation hardness measured for the thick duplex coating were higher than the ion nitrided coupon but lower than bare Haynes 25 (Table 2). Deposition of the Cr-N(ss)/Cr_2N coatings on the compliant, iron-rich surface layer of the nitrided coupons resulted in a duplex coating with a nano-indentation hardness that is lower than Cr-N(ss)/Cr_2N coatings deposited on bare Haynes 25. The grading in hardness/modulus, and use of the nitride layer to support the multilayer Cr-N(ss)/Cr_2N coating results in an attractive architecture for the duplex coating. Nano-indentation and scratch values for the low-pressure nitrided, duplex coating are comparable to the thin dual layer Cr-N(ss)/Cr_2N coating on Haynes 25, see Table 2.

5. Wear Test Results

5.1. 4-ball wear tests

Weight change results for the cups, intermediate balls, drive ball, and separator coupons are summarized in Figures 5a, 5b, 5c, and 5d, respectively. The weight loss values for the thin Cr_2N/Cr-N(ss) coated cups, intermediate balls, and separators were the lowest. Maximum wear depth measurements for the thin Cr_2N/Cr-N(ss) coated cups were also among the lowest, see Figure 6a. Comparison of pre-test and post-test profiles for the thin Cr_2N/Cr-N(ss) coated cups

show in Figure 6b that the volume and true depth of wear was significantly less than the uncoated cup (Figure 6c). The wear depth values given in Figure 6a for the thin Cr_2N/Cr-N(ss) coated cups are an overestimate due to some apserities on the as-received surface [1,2]. The majority (~99%) of the wear was smooth with no damage other than a few small regions, as shown in Figure 6d. The thin Cr_2N/Cr-N(ss) coated intermediate balls exhibited little wear, negligible decrease in coating thickness, and no coating deadhesion over the majority (~99%) of the surface, with the exception of small regions (Figure 6e). Ball-on-ball contact between the coated Haynes 25 drive ball and coated Stellite 3 intermediate balls results in high-stresses that produced substrate deformation on the softer Haynes 25 drive ball, which resulted in coating deadhesion and higher wear for one of the thin Cr_2N/Cr-N(ss) coated drive balls in comparison to the uncoated drive ball. These results indicate that the thin Cr_2N/Cr-N(ss) coating cannot endure ball-on-ball contact at high stresses when substrate deformation occurs.

The weight loss for the ion nitrided and thin duplex coated cups and intermediate balls were comparable to or higher than the uncoated cups and balls. However, less wear was observed for separators with the ion nitrided or thin duplex coated coupons. High stress, ball-on-ball contact resulted in plastic deformation of the Haynes 25 drive ball, which resulted in coating failure and a higher wear rate for the ion nitrided and thin duplex coated drive ball coupons. Post-test examinations showed that the ion nitride layer and thin duplex coating were adherent on the cup and intermediate balls with little wear [1,2]. The only wear observed on ion nitrided and thin duplex coated specimens was the smoothing of surface asperities, which resulted in a decrease in surface roughness [1,2]. As previously discussed, ion nitriding produces a large increase in surface roughness, and fracturing of asperities during the 4-ball wear test results in a higher weight loss than the uncoated substrates. Since the thin duplex coating is produced by deposition of thin Cr_2N/Cr-N(ss) layers on the rough ion nitrided surface, the wear behavior of the ion nitrided and thin duplex coated coupons was similar. Modification of the ion nitriding parameters to produce a smoother surface should improve the 4-ball wear resistance. Only the use of the thin Cr_2N/Cr-N(ss) coating,

which produced a negligible change in surface roughness after coating, provided a significant improvement in wear resistance for the 4-ball wear test.

5.2. Pin-on-Disc Wear Tests

The general sliding wear resistance of the Cr-N(ss)/Cr_2N coating and a 9 μm thick, monolithic tungsten coating was evaluated using a pin-on-disc test [2]. Results of this testing are summarized in Table 3. A test of the uncoated controls was terminated early due to high torque and friction values, see Table 3. The tip of the uncoated Stellite 3 pin was worn flat and Haynes 25 wear debris was adhesively transferred from the disc to the pin (Figure 7a), which likely produced the high friction/torque values. Deep grooves are observed on the uncoated Haynes 25 disc in Figure 7b.

Longer run times, and lower torque and friction values were observed for the self-mated Cr-N(ss)/Cr_2N coated specimens compared to the uncoated coupons. Although high-stress, point contact resulted in the tip of the Cr-N(ss)/Cr_2N coated pin being worn off, the wear damage of the Cr-N(ss)/Cr_2N coated pin shown in Figure 7c was less severe than the uncoated pin with no adhesive transfer observed. Little wear and surface roughening was observed on the Cr-N(ss)/Cr_2N coated disc in Figure 7d compared to the uncoated Haynes 25 disc. The friction coefficient and torque for the self-mated tungsten coating tests were comparable to the self-mated Cr-N(ss)/Cr_2N coating tests, but the run time was short for one test. The wear damage was more severe for the tungsten coated coupons than the Cr-N(ss)/Cr_2N coated coupons.

Mixed couple tests consisting of tungsten coated pins/discs mated with Cr-N(ss)/Cr_2N coated discs/pins were also performed. The torque and friction values for the mixed couple tests were comparable to the self-mated Cr-N(ss)/Cr_2N coated tests, but the run times were shorter and a greater amount of wear damage was observed. The pin-on-disc results indicate that the self-mated Cr-N(ss)/Cr_2N coated specimens had the best wear performance, which is consistent with the results observed in the 4-ball wear test.

5.3. Rolling Contact (RC) Wear Tests

Quantitative wear test data from the rolling contact (RC) wear tests are presented in

Table 4. All of the eight candidate coatings listed in Table 2 were subjected to at least one 48h test phase of rolling contact wear testing. Four of the eight coatings (thick duplex coating, low-pressure duplex coating, ZrN coating, and plasma carburizing) exhibited an unacceptable level of deadhesion. Four other coating candidates were adherent and had significantly less wear than the uncoated controls (thin and thick Cr-N(ss)/Cr_2N coatings, ion nitriding, and thin duplex coating). A second set of these coatings were tested for 48h followed by an additional 96h test phase for a total test time of 144h.

A cumulative plot of roller weight change data for the four best performing coatings and the uncoated reference material is shown in Figure 8. The ion nitriding surface modification, thin duplex coating, and thick four-layer Cr-N(ss)/Cr_2N/Cr-N(ss)/Cr_2N coating were all extremely effective in reducing Haynes 25 roller wear. The thin dual-layer Cr-N(ss)/Cr_2N coated rollers showed higher weight losses which were only about 2.5 times lower than untreated rollers after 144 hours of testing. This is because the coating was worn away sometime during the second 96 hour test phase and the wear rate reverted back to the higher values exhibited by the uncoated reference materials. The average change in surface roughness for the uncoated rollers and bushing after testing was generally high for the uncoated coupons. As discussed below, a significant amount of roller to bushing adhesive material transfer occurred between the uncoated materials. The bushing weight change results in Table 4 are therefore not a valid measurement of uncoated specimen wear.

5.3.1. Post-test examinations of uncoated RC specimens

A deep wear groove was observed on the uncoated Haynes 25 roller after the RC tests (Figure 9a), but the right side of the roller was unworn and the original machining marks could be resolved. Using the unworn edge of the roller as a reference plane, the wear depth was measured from metallographic cross-sections (see Table 5 and Figures 10a and 11). Assuming the average wear depth corresponds to a volume of material removed from the edge of the roller (density for Haynes 25 = 8.9 g/cm^3), the average wear depth measured for the 48h (21.8 μm)

and 48h + 96h (58.2 μm) test gives a calculated weight loss of 37.1 mg (48h) and 98.5 mg (48h + 96h), respectively, which is less than a factor of 1.3 higher than the actual weight loss in Table 4. Considering the non-uniform wear depth and the unworn edge at the side of the roller, these calculated weight losses are in close agreement with the measured weight change.

The post-test surface roughness of the 17-4 PH bushings that were mated with the uncoated Haynes 25 rollers was fairly high, see Figure 12a. The bushing was covered with adherent cobalt-rich debris that was transferred from the Haynes 25 rollers. Metallographic cross-sections in Figure 11b show that the thickness of the cobalt-rich wear debris ranged from 6.4 to 50.8 μm. The presence of this adhesively transferred material tended to invalidate the weight change measurements.

One measure of wear is the post-test thickness of the land of the bushings (see Table 6 and Figure 13). The initial land thickness (0.254 cm ± 0.005 cm, see Figure 1b) increases to 0.307 cm after 48h and 0.356 cm after 48h + 96h. The wear of the bushing mated with the uncoated roller was slightly higher than the bushings mated with the ion nitrided and thick four-layer Cr-N(ss)/Cr_2N coating and more comparable to the bushings mated with the thin Cr-N(ss)/Cr_2N coated and thin duplex coated roller, see Figure 13. These differences in bushing wear are not significant.

5.3.2. Thin dual-layer Cr-N(ss)/Cr_2N coating

The weight changes and dimensional changes for the thin (0.9 μm) Cr-N(ss)/Cr_2N coated rollers were significantly less than the uncoated roller after the 48h RC test (see Figures 8 and 11). However, SEM and metallographic examinations indicated that the coating was damaged and worn through to the base material in some regions. Although the coating had protected the majority of the roller surface during the 48 RC test and significantly lowered the wear rate, the coating was not thick enough to survive the high-stress wear contact for a longer period of time. The thin Cr-N(ss)/Cr_2N coating layer was fully worn away after the 48h + 96h RC test. Figure 14a shows that a thin region of unworn coating area had remained at the edge of the roller, and a groove had been worn into the Haynes 25 roller that is similar in shape to the uncoated roller

(Figure 10a) with a lower wear depth. Although the thin Cr-N(ss)/Cr_2N coating was worn away in the 48h + 96 RC test, the rate of wear, or slope of wear depth versus time (Figure 11) or weight change versus time (Figure 8), are less than the uncoated rollers. The exact point at which the coating was worn away during the 96h RC test period could not be defined, but the lower wear rate for the thin Cr-N(ss)/Cr_2N coated rollers indicates a graceful wear-through of an adherent coating that produces only fine wear debris does not increase the base wear rate of Haynes 25.

Based on measurements of bushing wear and surface roughness after the 48h RC test in Figure 13, bushings mated with the thin Cr-N(ss)/Cr_2N coated roller wore less than the bushings mated with uncoated rollers. However, even though the coating was worn away from the Haynes 25 roller after the longer 48h + 96h RC test, Figure 13 shows that the bushing wear was only slightly higher than the uncoated bushing. The coating had protected the Haynes 25 roller for at least 1/3 (48h) of the 48h + 96h RC test, and the amount of Co-rich debris observed on the bushing surface was less than the uncoated bushing (see Figure 14b). The wear through of the thin Cr-N(ss)/Cr_2N coating during the 48h + 96h RC test did not increase the roller wear. The fine abrasive debris from the thin coating did result in slightly higher bushing wear when compared to the uncoated test couples, but the differences in wear not significant.

5.3.3. Thick 4-layer Cr-N(ss)/Cr_2N Cr_2N/Cr-N(ss) coating

The thick 4-layer Cr_2N/Cr-N(ss)/Cr_2N/Cr-N(ss) (thick Cr-N) coated rollers were generally smooth after the 48h and 48h + 96h RC tests with little debris. However, notable regions of coating deadhesion or pocks were observed on about 5% to 10% of the surface (see Figures 9b and 15a). The highest amount of coating pocking (about 10% of surface) and coating micro-cracking was observed after the 48h + 96h RC test. SEM examinations showed that many of the pocks were only one or two layers deep, while some were the result of full removal of the coating which exposed the Haynes 25 roller. The fine coating micro-cracks observed on the surface of the roller (Figure 9b) and roller cross-section (Figure 15a) resulted from subsurface deformation, but the coating was generally adherent. The micro-cracking was localized on the

right side of the roller in Figure 9b, which indicates that higher stresses (and greater amounts of sliding) occurred on this section of the roller.

Although a limited amount of coating damage (pocking and micro-cracking) had occurred on the thick Cr-N coated roller after the RC test, this coating exhibited the lowest wear rate (see Figures 8 and 11). The use of a thicker coating with soft inner-layers to match the coating modulus/hardness with the base material appears to decrease the level of interfacial stresses that result from high stress wear contact. The high stresses did result in some coating micro-cracking and pocking on limited regions of the roller, suggesting that a better match in hardness/modulus could provide further improvements in the resistance of the coating to wear damage.

The wear surfaces of bushings that were mated with thick Cr-N coated rollers appeared much smoother with much less debris than the bushing mated with uncoated rollers, see Figures 12 and 15b. The thickness of the worked zone on the surface of the bushing mated with the thick Cr-N coating (Figure 15b) was about half that observed for the bushings mated with the uncoated rollers (Figure 10b). The surface of the bushings was covered with a thin (~1 μm) layer of material that was not observed on bushings that had been mated with uncoated rollers. This layer of material likely results from wear contact with the Cr_2N/Cr-N(ss) coating, and further analysis will be needed to characterize this layer. The formation of this thin (~1 μm) layer on the bushing material may contribute to the significantly lower level of bushing and roller wear.

5.3.4. Ion nitriding surface modification

The ion nitriding rollers appeared smooth after the 48h and 48h + 96h RC test with no evidence of wear damage, see Figure 9c. The rollers were covered with some iron-rich wear debris from the 17-4 PH bushing. Surface SEM examinations and metallographic cross-section showed that the nitride layer remains tightly adherent, with some wear and a minor amount of micro-cracking. This indicates that the relatively thick and adherent nitride layer, with a good match in modulus/hardness to the base material, results in lower interfacial stress under the

high-stress contact produced in the RC test. However, the nitride layer was worn through to the Haynes 25 base metal in one region of the roller after the 48h + 96h RC test (see Figure 16a). The initial thickness of the nitride layer, which is a (Co,Cr,W,Ni,Fe)N compound, and the thick four-layer Cr_2N/Cr-N(ss)/Cr_2N/Cr-N(ss) coating are similar (Table 2), but the wear rate of the nitride layer was much higher.

The wear surfaces of the bushings that were mated with the ion nitriding rollers were much smoother than the bushings mated with the uncoated roller, see Figure 12c. SEM examinations of the bushing surfaces show a low amount of wear debris that contained some cobalt (< 6 weight%), which indicates that this wear debris originated from the nitride layer. The metallographic cross-section of the bushings mated with the ion nitriding rollers (Figure 16b) confirmed that some transfer of wear debris had occurred. However, the lowest level of bushing wear was measured for bushings mated with ion nitriding rollers (see Table 6 and Figure 13).

5.3.5. Thin duplex coating

Post-test surfaces of the thin duplex coated rollers were fairly smooth in the center, where pure rolling wear occurs, and rougher at the edges of the roller with some debris, (see Figure 9d). The greater amount of sliding experienced at the edges of the roller produced a slight amount of scuffing damage to the coating. Metallographic cross-sections of the t-duplex coated rollers showed that the outer Cr_2N/Cr-N(ss) layers were fully intact on the outer regions of the roller, but some minor wear damage was observed in the central region of the rollers. The underlying nitride layer was virtually intact and little coating wear was observed (Figure 11 and Tables 5 and 7). Some coating micro-cracks were observed (Figure 17a), but the coating remained tightly adherent, spalling of the nitride layer was not detected, and very low wear rates were observed (Figures 8 and 11). The grading in modulus/hardness for the thin duplex coating with the ion nitride layer providing the needed support for the outer Cr_2N/Cr-N(ss) layers reduced the interfacial stresses that result from high stress wear contact. Furthermore, the presence of the outer Cr_2N/Cr-N(ss) layers on the thin duplex coatings results in a significantly lower wear

rate than that observed for the nitride layer alone (Tables 4 and 5). The low wear rates observed for the thin duplex and thick Cr_2N/Cr-N(ss)/Cr_2N/Cr-N(ss) coated rollers indicates that an outer Cr_2N/Cr-N(ss) layer produces a low wear rate in contact with 17-4 PH.

The wear surface of the bushings that were mated with the thin duplex coated rollers were smoother with significantly less debris than observed for the bushings mated with an uncoated roller (see Figure 12d). Metallographic sections of the bushings (Figure 17b) show a lower depth of working than bushings that were mated with uncoated rollers. A thin transferred surface layer (~1 μm, see Figure 17b) was similar in appearance to the layer observed on bushings which were mated with the thick four-layer Cr_2N/Cr-N(ss)/Cr_2N/Cr-N(ss) coated rollers (Figure 15b). This suggests that the wear between the Cr_2N/Cr-N(ss) coating and 17-4 PH bushings produces a transferred layer, which appears to decrease the roller and bushing wear. However, the as-coated surface of the thin duplex coated roller was fairly rough [1,2], and the wear and fracturing of surface asperities appears to result in a slightly higher amount of bushing wear than observed for the uncoated bushing (Figure 13) .

5.3.6. Other Coating Candidates

Four coating candidates exhibited poor performance in the first 48h RC test (thick duplex coating, low-pressure duplex coating, ZrN coating, and plasma carburizing).

The weight losses for the thick (6 μm) duplex coated rollers were significantly less than the uncoated roller, but the bushing weight losses were among the highest observed. The underlying nitride layer of the thick duplex coated roller was tightly adherent, but the spalling of the outer Cr_2N/Cr-N(ss) layers was unacceptably high. The deposition of a thicker Cr_2N/Cr-N(ss) coating generally produces higher residual stresses. The thick (11 μm) four-layer Cr_2N/Cr-N(ss)/Cr_2N/Cr-N(ss) coating had been deposited on bare Haynes 25 with excellent adhesion. However, low adhesion was observed for the 6 μm thick Cr_2N/Cr-N(ss) coating which was deposited on the nitride layer to form the thick duplex coating. The higher surface roughness and iron-rich surface layer on the ion nitrided surface, coupled with the higher residual stresses

resulting from the deposition of a thicker coating, probably resulted in low coating adhesion for the thick duplex coating in the RC test.

Based on weight loss measurements of the rollers and bushings in Table 4, the low-pressure duplex coated rollers and bushings exhibited low wear after the 48h RC test. However, a significant fraction of the coating was worn through or spalled off after the test. Although scratch adhesion testing indicated that the low-pressure duplex coating had excellent adherence on Haynes 25 (Table 2), the diffusion zone was too thin ($\approx 1\mu m$) to provide the support needed for the very thin (0.7 μm) outer Cr_2N/Cr-N(ss) layers. Consequently, the high stress wear contact associated with the RC test resulted in high interfacial stresses and coating deadhesion.

The weight change of the ZrN coated rollers and bushings was significantly higher than the other coating candidates (Table 4). The higher wear rate resulted from the significant spalling which occurred during the RC test. A high miss-match in modulus/hardness between the ZrN coating and the Haynes 25 base material (Table 2) resulted in high interfacial stresses and coating deadhesion from the high contact stresses. Although very low amounts of weight loss were measured for the plasma carburized rollers and bushings, gross deadhesion of the plasma carburized layer was observed. Because the carbon + oxygen (soot) layer produced by plasma carburizing was soft and lubricious in nature, the extensive deadhesion of this layer did not produce a high wear rate. The non-adherent layer produced by this plasma carburizing process is not a viable wear coating.

6.0 Summary

The differences in stiffness (or modulus/hardness) between the coating and cobalt-base substrate must be minimized to enable the use of a wear resistant coating in high-stress applications. Four promising coating approaches have been identified using scratch adhesion and indentation testing: (1) use of a thin coating with hard Cr_2N and less-stiff Cr-N(ss) layers, (2) the use of a thick, four-layered coating with a 4 μm inner layer of Cr-N(ss) / 1 μm layer of Cr_2N / 4 μm layer of Cr-N(ss) / 1 μm outer layer of Cr_2N, (3) a duplex approach of ion nitriding to harden

the subsurface followed by application of a thin, dual-layered Cr_2N/Cr-N(ss) coating, and (4) use of ion nitriding alone. These four coating candidates exhibited the best results in a high stress RC wear test, and were subjected to a second 48h + 96h wear test. The thin dual-layer Cr-N(ss)/Cr_2N coating was worn away during the 96h period of the 48h + 96h RC test, but the wear rate was significantly less than the uncoated roller. This result indicates that if an adherent coating is gracefully worn away producing only fine debris, then accelerated wear of the base metal will not be observed. The ion nitride layer was adherent and protected the roller, but wear through was observed after the 48h + 96h RC test. Therefore, ion nitriding alone does not provide the most adequate protection. The thick Cr-N(ss)/Cr_2N/Cr-N(ss)/Cr_2N coating exhibited the lowest wear of all candidates evaluated, but limited pocking or deadhesion of the coating was observed on about 10% of the coated surface. A low wear rate was observed for the thin duplex coating, which consists of a thin dual-layer Cr-N(ss)/Cr_2N coating on top of an ion nitride layer, and the coating was adherent, with only slight wear damage of the outer Cr-N(ss)/Cr_2N layers. The thin duplex coating provided the best wear protection for a highly loaded surface.

Based on weight change, profilometry measurements, and post-test examinations after 4-ball wear testing, thin dual-layer Cr_2N/Cr-N(ss) coated specimens exhibited a significantly lower wear rate than similar uncoated specimens. More importantly, the thin Cr_2N/Cr-N(ss) coatings were adherent on the Stellite 3 intermediate balls and Haynes 25 cups, and prevented the wear of the cobalt-base substrate. Based on friction values, torque values, run time, and SEM examinations after pin-on-disc testing, self-mated Cr_2N/Cr-N(ss) coated pins and disks exhibited the best wear resistance. Results from the 4-ball and pin-on-disc tests show that the use of self-mated, Cr_2N/Cr-N(ss) coated substrate significantly improves the wear resistance of cobalt-base alloy substrates.

Acknowledgments

This work was performed under USDOE Contract DE-AC11-98PN38206. The technical comments and contributions of J. L. Hollenbeck and S.A. Shiels are appreciated.

References

[1] B.V. Cockeram, Surf. Coat. Technol. 120/121 (1999) 509.

[2] B.V. Cockeram, "Development of Wear-Resistant Coatings for Cobalt-base Alloys", Available as WAPD-T-3254, DOE/OSTI (Oak Ridge TN, 1999).

[3] *Friction, Lubrication, and Wear Technology*, Materials Handbook, Volume 18, ASM International, Materials Park, OH, 1992, p. 758.

[4] E.K. Ohriner, T. Wada, E.P. Whelan, and H. Ocken, Met. Trans., 22A (1991) 983.

[5] L. Zheng and S. Ramalingam, J. Vac. Sci. Techol. A, 13 (1995) 2390.

[6] L. Zheng and S. Ramalingam, Surface and Coatings Technology, 81 (1996) 52.

[7] *The Rolltact Test Machine*, Industrial Tectonics Report No.106, Industrial Tectonics, Inc., Compton, CA, 1988.

[8] W.C. Oliver and G.M. Pharr, J. Mater. Res., 7(6) (1992) 1564.

[9] A.J. Perry, J. Valli, and P.A. Steinmann, Surf. and Coatings Technol., 36 (1988) 559.

[10] T.Y. Tsui, G.M. Pharr, W.C. Oliver, Y.W. Chung, E.C. Cutiongco, C.S. Bhatia, R.L. White, R.L. Rhoades, and S.M. Gorbatkin, MRS Res. Soc. Symp. Proc., 356 (1995) 767.

[11] P.H. Nowill, Proceedings of 2nd International Conference on Ion Nitriding/Ion Carburizing, ASM International, Materials Park, OH (1990) 29, 175.

[12] Surface Engineering, Materials Handbook, Volume 5, ASM International, Materials Park, OH (1994) 737.

Table 1. Nominal composition of base materials used in coating scratch adhesion, rolling contact wear, 4-ball wear, and pin-on-disc wear testing
[Compositions in Weight%]

Alloy / Substrate	Co	Cr	W	Ni	Mn	C	Fe	Si	S	P	Other	Hardness HRC
Haynes 25 Flats, Rollers, and Discs	Bal	20.7	14.6	10.1	1.42	0.12	2.7	0.22	<.002	0.008	---	47
Haynes 25 Cups	Bal	20.4	14.6	10.1	1.43	0.09	2.17	0.16	<.002	0.013	---	52
Haynes 25 Balls	Bal	20.1	15.2	10.1	1.43	0.10	0.9	0.1	.0002	0.01	---	46
Stellite 3 Balls and Pins	Bal	30.04	11.82	1.82	0.35	2.20	1.66	0.81	0.012	0.012	.21 Mo .05 Ti	53
17-4 PH Separator	--	16.5	--	3.4	0.5	0.04	Bal	0.5	0.01	0.01	3.4 Cu 0.3 Nb	36

Table 2. Summary of coating/surface modifications and results of hardness, scratch adhesion, and nano-indentation tests.

Coating/ Surface-Modification, Vendor	Average Thickness ± Standard Deviation [μm]	Coating Hardness [VHN or KHN]	Scratch Adhesion Critical Load Value [kg]	Nano-indentation Test Results	
				Critical Load Value [mN]	Hardness / Modulus [GPa/GPa]
Uncoated Haynes 25	N/A	200-400 KHN	Not Measured	N/A	7.4 / 258.5
Coating Candidates Used for Rolling Contact Wear Testing (deposited on flats and rollers)					
Four-layer Cr-N(ss)/Cr_2N Coating, ACT	10.4 ± 1.1	1930 VHN	7.5	NF	14.2 / 270.4
TiN Coating, GM	2-3	2500-3000 VHN	2.0 – 3.0	15	25.7 / 400.5
ZrN Coating, PST	8.9 ± 0.9	2150 VHN	5.1	15 – 17	26.0 / 405.9
Plasma Carburizing, SC	13.8 ± 4.2	N/A	Not Measured	8 – 10	N/A
Low-pressure Duplex Coating, ACT	0.6 ± 0.2 Diff. Zone = 1.1 ± 0.3	1670 VHN	7.0 – 8.0	23	14.2 / 258.5
Thick Duplex Coating, AHT + ACT	Cr-N(ss)/Cr_2N = 5.8 ± 0.6 Nitride = 11.7 ± 1.3	1990 VHN	4.5 – 5.5	NF	5.8 / 183.1
Coating Candidates Used for both 4-ball Wear Testing and Rolling Contact Wear Testing (deposited on flats, rollers, balls, and cups)					
Dual-layer Cr-N(ss)/Cr_2N Coating, ACT	0.9 ± 0.2	1930 VHN	5.0 – 7.0	22.0	19.3 / 290.5
Ion Nitriding, AHT	11.7 ± 1.3	700-1100 KHN	Not Measured	NF	1.4 / 66.7
Thin Duplex Coating, AHT + ACT	Cr-N(ss)/Cr_2N = 3.0 ± 1.2 Nitride = 11.7 ± 1.3	1970 VHN	5.0 – 5.5	NF	Not Measured
Candidates Used for Pin-on-Disc Testing (deposited on pins and discs)					
Dual-layer Cr-N(ss)/Cr_2N Coating, ACT	2.5	1910 VHN	3.5	Not Measured	Not Measured
Tungsten Coating, ACT	9.0	1600 VHN	Not Measured	Not Measured	Not Measured

Notes:
1. ACT = Advanced Coating Technology Group, Materials Technology Laboratory, Northwestern University, Evanston, IL.
2. AHT Corp. = Advanced Heat Treat Corporation, Waterloo, IA.
3. PST = Praxair Surface Technologies, Inc., Indianapolis, IN.
4. SC = Surface Combustion Corporation, Maume, OH.
5. GM = General Magnaplate, Linden, NJ.
6. NF = No Coating Failure Observed.
7. N/A = Could Not Be Determined.
8. Hardness and adhesion measurements were made on Haynes 25 flats.

Table 3. Pin-on-disc wear test results.

Test Number	Pin Coating / Disc Coating	Start Friction Coefficient	Maximum Friction Coefficient	Start Torque [kg-cm]	Maximum Torque [kg-cm]	Run Time [Minutes]
1	Uncoated/Uncoated	0.388	0.495	2.89	4.35	12
2	CrN/CrN	0.256	0.402	3.47	7.55	30
3	CrN/CrN	0.274	0.420	4.06	4.93	6
4	W/W	0.327	0.455	5.33	7.27	30
5	W/W	0.072	0.293	1.44	4.95	0.7
6	W/CrN	0.272	0.477	4.26	7.61	4
7	W/CrN	0.329	0.475	5.22	7.55	0.3
8	CrN/W	0.109	0.514	5.53	7.29	0.3
9	CrN/W	0.146	0.219	2.31	2.89	14

Notes: 1. Tests performed at Advanced Coating Technology (ACT) group, Northwestern University.
2. Tests performed in ambient temperature distilled water.
3. CrN = 2.5 μm thick chromium-nitride coating with a 3:2 ratio of Cr-N(ss) to Cr_2N layers.
4. W = 9 μm thick tungsten coating.
5. The pin was Stellite 3, the disc was Haynes 25.

Table 4. Summary of rolling contact wear test results.

Coating	Test Time [hr][1]	HAYNES 25 ROLLER			17-4 PH BUSHING		
		Weight Change [mg]	Avg. Wt.[2] Change [mg]	Avg. [3] Surface Change [Å]	Weight Change [mg]	Avg. Wt.[2] Change [mg]	Avg. [3] Surface Change [Å]
Uncoated Reference	48	-36.9, -33.6, -29.4	-33.3	10,000	-20.0, -15.0	-17.6	23,300
	48	-36.6, -31.4, -37.3	-35.1	12,700	-23.2, -17.8	-20.5	24,500
	48	-30.2, -27.8, -30.9	-29.6	--	-15.9, -22.8	-19.4	--
	48	-29.0, -22.9, -21.6	-24.5	3,380	-15.9, -19.3	-17.6	16,800
	48 + 96	-47.6, -50.0, -50.5	-49.4	1,780	-45.3, -39.8	-42.6	3,100
Ion Nitriding	48	-1.4, -1.2, -1.0	-1.2	-3,280	-81.7, -83.7	-82.7	7,700
	48	-0.9, -0.6, -1.3	-0.9	-4,950	-82.9, -80.8	-81.8	7,670
	48 + 96	-3.1, -3.0, -5.0	-3.7	4,390	-33.2, -30.5	-31.8	3,810
Dual-layer Cr-N(ss)/Cr_2N Coating	48	-0.7, -1.0, -0.7	-0.8	2,260	-91.3, -87.9	-89.6	9,220
	48	-3.6, -3.5, -2.3	-3.1	2,440	-118.4, -117.3	-117.8	15,000
	48 + 96	-21.6, -34.2, -30.1	-28.6	8,970	-156.2, -139.6	-147.9	19,900
Thin Duplex Coating	48	-0.3, -0.3, -0.4	-0.3	711	-145.9, -135.7	-140.8	7,320
	48	-0.59, -1.24, -1.18	-1.00	-1,350	-139.1, -136.6	-137.8	11,000
	48 + 96	-1.04, -1.35, -1.97	-1.45	3,000	-151.2, -202.7	-176.9	2,210
Four-layer Cr-N(ss)/Cr_2N Coating	48	-0.2, 0.1, -0.1	-0.1	-2,720	-79.0, -75.3	-77.1	6,350
	48	0.0, -0.3, 0.0	-0.1	4,620	-85.8, -87.7	-86.8	7,320
	48 + 96	-1.2, -1.0, -1.0	-1.1	1,350	-77.9, -89.9	-83.9	4,570
Plasma Carburizing	48	-1.6, -1.5, -0.2	-1.1	-3,380	0.5, 0.4	+0.45	-660
ZrN Coating	48	-9.3, -12.3, -9.6	-10.4	1,020	-184.6, -196.0	-190.3	11,700
Low-pressure Duplex Coating	48	-0.2, -0.3, -1.0	-0.5	-483	-72.5, -73.7	-73.1	8,000
Thick Duplex Coating	48	-1.8, -2.9, -1.4	-2.0	686	-152.4, -154.0	-153.2	8,130

Notes:

1. The rows with a test listed as 48h followed by a row with a test listed as 48h + 96h are the same set of coupons test for 48h in the first phase followed by a second 96h test for a total test time of 144h.
2. Average weight (Wt.) change data are the average for the 3 rollers and 2 bushings in each test.
3. Surface roughness change calculated as [(Post-test roughness) – (Pre-test roughness)]. Negative values therefore indicate a smoothing of the wear surfaces. Measurements were taken at three locations (120° interval) on each roller and bushing test surface. Average values were determined from 9 readings on the 3 rollers and 6 readings on the two bushings.

Table 5. Summary of wear depth measurements for rollers after Rolling Contact (RC) wear testing.

Candidate	Duration of Test [hours]	Average Wear Depth ± Standard Deviation [μm][1]	Range of Wear Depth [μm][1]
Uncoated (Reference)	48	21.8 ± 5.1	34.0 to 14.0
	48 + 96	58.2 ± 11.7	82.0 to 39.9
Thin dual-layer Cr_2N/Cr-N(ss) Coating	48[2]	0.3 ± 0.8	1.3 to 0.0
	48 + 96	23.1 ± 6.6	41.9 to 14.0
Ion Nitriding Surface Modification	48[2]	1.8 ± 1.3	3.8 to 0.3
	48 + 96[2]	5.6 ± 3.6	10.7 to 0.8
Thin Duplex Coating	48[2]	0.3 ± 0.4	2.0 to 0.0
	48 + 96[2]	2.0 ± 1.4	5.1 to 0.1
Thick four-layer Cr_2N/Cr-N(ss)/ Cr_2N/Cr-N(ss) coating	48[2]	0.1 ± 2.8	10.7 to 0.0
	48 + 96[2]	0.6 ± 3.6	10.7 to 0.0

Notes:

1. All measurements were taken from metallographic sections.
2. These coatings were generally intact, and the wear depth was estimated based on observed coating wear, i.e. original coating thickness (Table 2) minus post-test coating thickness (Table 7).

Table 6. Summary of wear tract measurements for uncoated 17-4 PH bushings after Rolling Contact (RC) testing.

Candidate	Duration of Test [hours]	Original Thickness of Bushing Land [cm]	Post-test Thickness of Bushing Land	
			Average ± Standard Deviation [cm]	Range of Values [cm]
Uncoated (Reference)	48	0.254	0.307 ± 0.005	0.312 to 0.300
	48 + 96	0.254	0.356 ± 0.005	0.366 to 0.351
Thin dual-layer Cr_2N/Cr-N(ss) Coating	48	0.254	0.281 ± 0.005	0.290 to 0.272
	48 + 96	0.254	0.376 ± 0.005	0.386 to 0.371
Ion Nitriding Surface Modification	48	0.251	0.300 ± 0.003	0.307 to 0.295
	48 + 96	0.254	0.310 ± 0.005	0.320 to 0.302
Thin Duplex Coating	48	0.251	0.307 ± 0.003	0.318 to 0.302
	48 + 96	0.254	0.373 ± 0.005	0.381 to 0.366
Thick four-layer Cr_2N/Cr-N(ss)/ Cr_2N/Cr-N(ss) coating	48	0.254	0.312 ± 0.003	0.318 to 0.295
	48 + 96	0.254	0.322 ± 0.003	0.328 to 0.318

Notes:

1. Measurements based on SEM surface examinations and metallographic sections.

TABLE 7. Summary of post-test coating thickness measurements after Rolling Contact (RC) testing.

Coating/ Surface-Modification	Duration of Test [hours]	Average Thickness ± Standard Deviation [μm]	Maximum Thickness [μm]	Minimum Thickness [μm]	Comments
Thin dual-layer Cr_2N/Cr-N(ss) Coating	48	0.56 ± 0.52	1.1	0.0	Coating thickness was difficult to measure. Coating wear through and fracture was observed on many regions.
	48 + 96	NA	NA	NA	Coating worn away.
Ion Nitriding Surface Modification	48	9.9 ± 1.3	11.5	8.0	Wear of the nitride layer was somewhat nonuniform.
	48 + 96	6.3 ± 3.5	11.0	0	Nitride layer was worn through at one location.
Thin Duplex Coating Treatment: (Ion Nitriding + Cr_2N/Cr-N(ss) coating)	48	12.8 ± 1.3	15.0	10.0	Measured values are for nitride layer + outer Cr_2N/Cr-N(ss) layer. Non-uniform wear. Cr_2N/Cr-N(ss) layer mostly intact.
	48 + 96	11.1 ± 1.4	13.0	8.0	
Thick four-layer Cr_2N/Cr-N(ss)/ Cr_2N/Cr-N(ss) Coating	48	10.6 ± 2.9	11.5	0	Little coating wear observed in regions where the coating was intact. Areas of coating deadhesion (pocks) were observed.
	48 + 96	10.0 ± 3.6	12.5	0	

Notes:

1. A reported minimum value of 0 indicates that regions of coating spalling to expose base material were observed.
2. All measurements were made from metallographic sections.

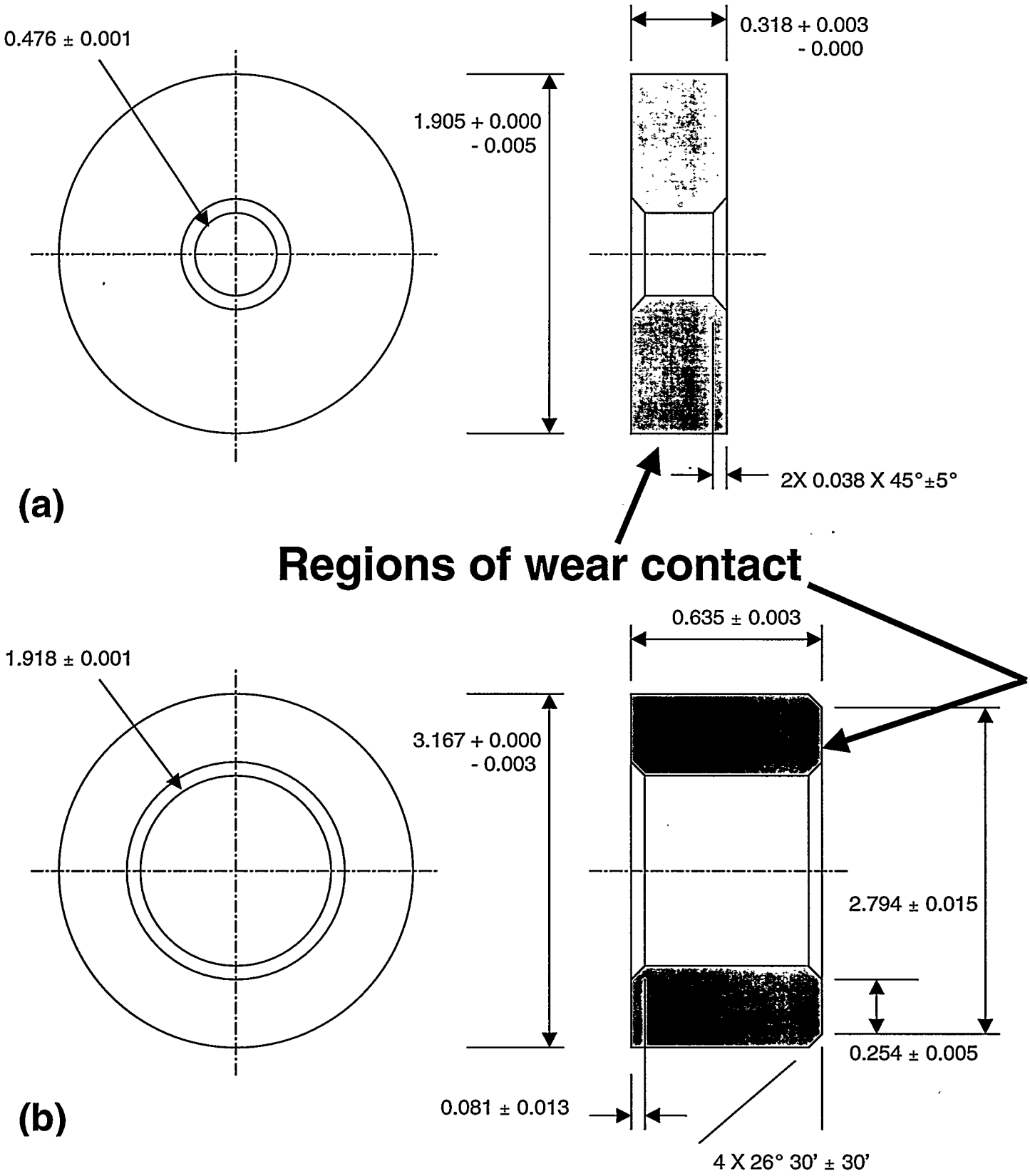

Figure 1. Schematic drawings of the specimens used in the Rolling Contact (RC) wear test: (a) Haynes 25 roller, and (b) 17-4 PH bushing. The regions of wear contact for the RC test are indicated. All dimensions are in cm.

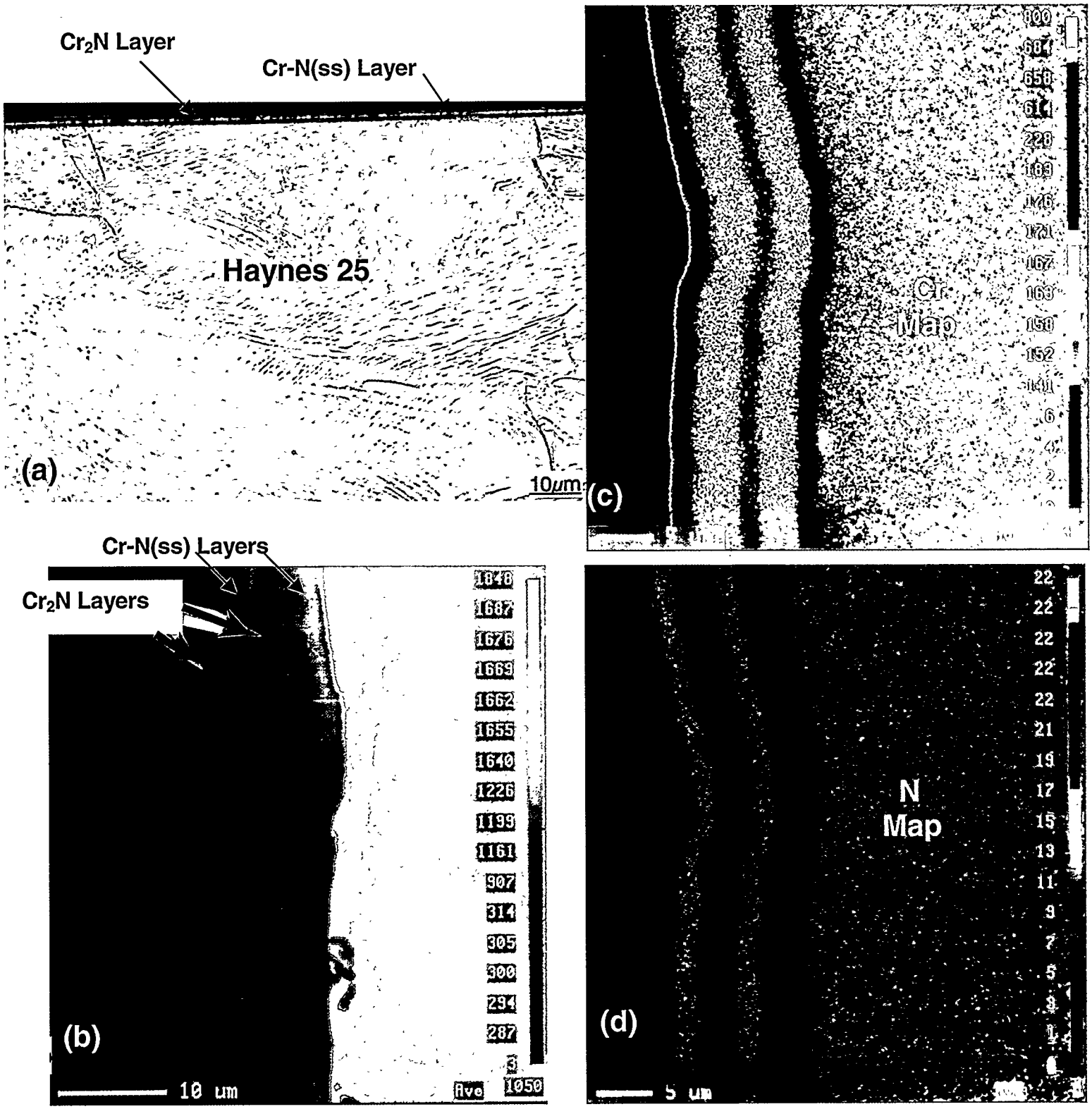

Figure 2. Cross-sectional metallography of multilayer chromium-nitride coatings deposited on Haynes 25: (a) optical metallography of thin, dual-layer Cr_2N/Cr-N(ss) coating (Mag=1,000X) after etching showing the thin Cr_2N and Cr-N(ss) layers, (b) SEM/BSE micrograph of thick, four-layer Cr_2N/Cr-N(ss)/Cr_2N/Cr-N(ss) coating showing the Cr_2N and Cr-N(ss) layers (Mag=2,000X), (c) chromium X-ray map of Fig. 2b, and (d) nitrogen X-ray map of Fig. 2b.

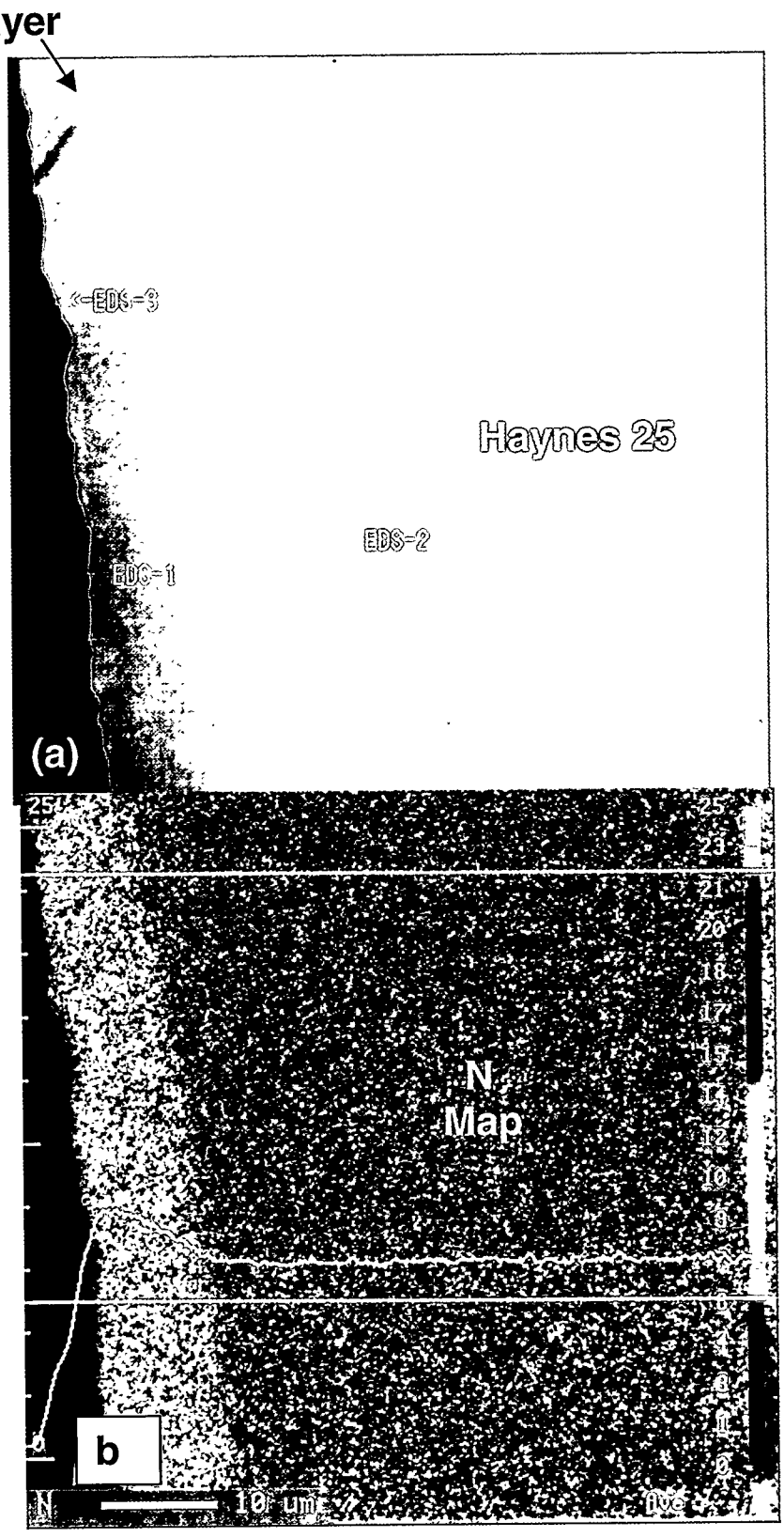

Figure 3. Cross-sectional metallography of the nitride layer produced by ion nitriding at 566°C for 48 hours: (a) SEM/BSE micrograph of the nitride layer grown on Haynes (Mag=1,500X), (b) nitrogen X-ray map of Fig. 3a, (c) optical micrograph of etched cross-section showing the diffusion zone and nitride layer (Mag=500X), (d) optical micrograph of etched section showing the nitride layer grown on Stellite 3 (Mag=1,000X), and (e) SEM image of the surface of ion nitrided Haynes 25 showing the iron-rich surface nodules and a nano-scratch indentation.

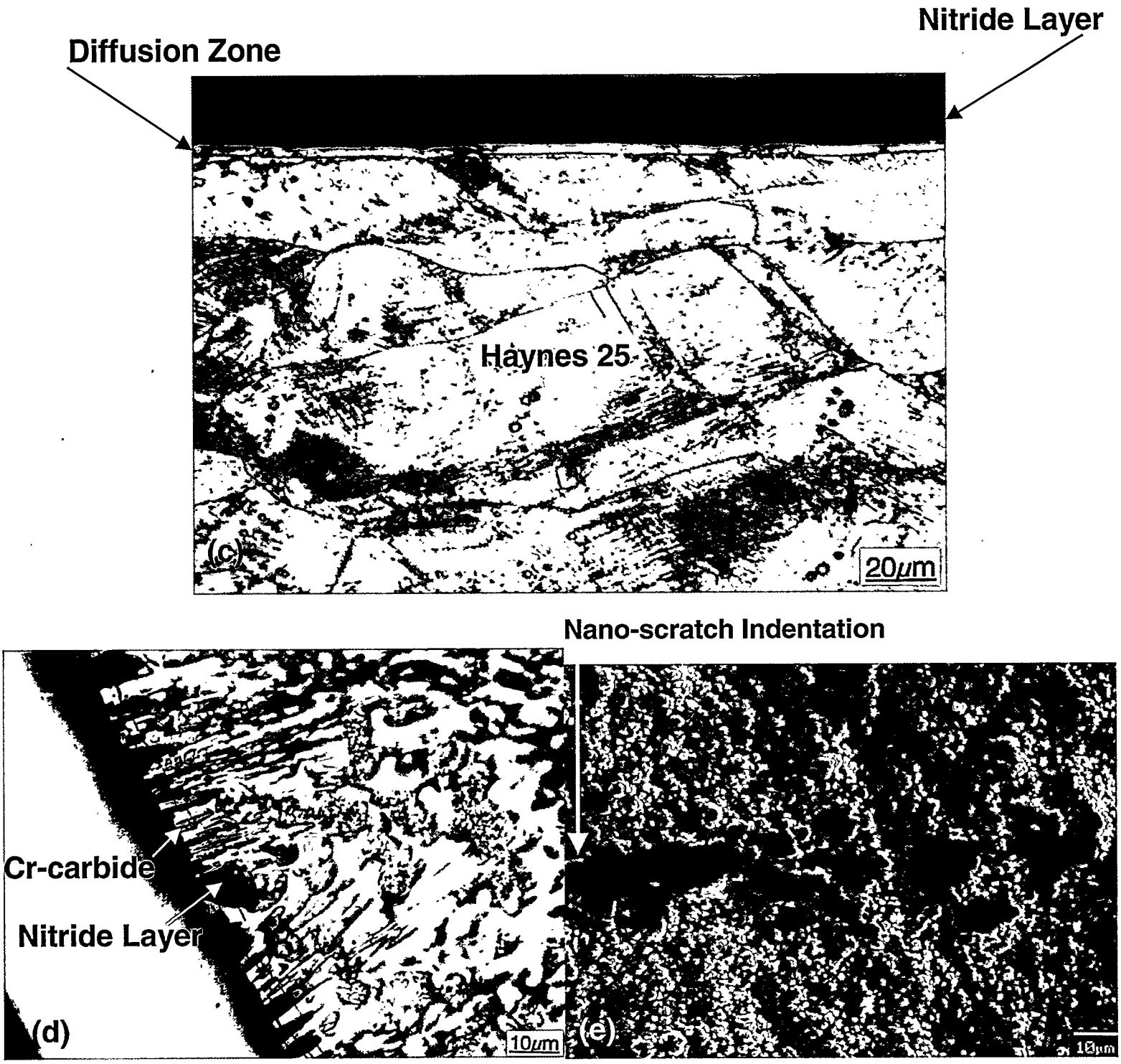

Figure 3. (Continued).

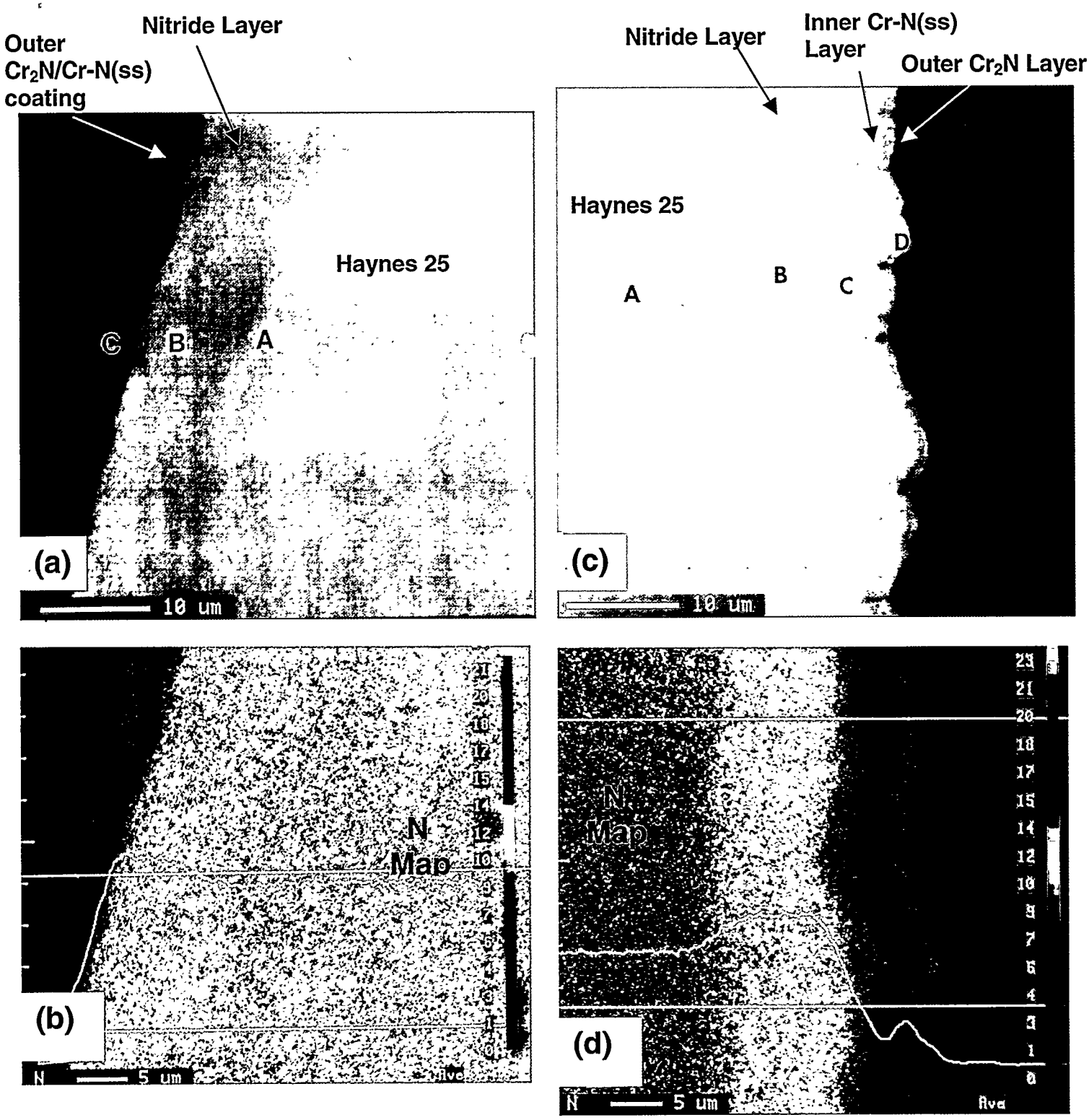

Figure 4. Metallographic section of duplex coatings deposited on Haynes 25: (a) SEM/BSE image of thin duplex coating (Mag.=2,000X), (b) nitrogen X-ray map of Figure 4a with a line profile, (c) SEM/BSE image of thick duplex coating at 2,000X magnification, and (d) nitrogen X-ray map of Figure 4c with a nitrogen line profile.

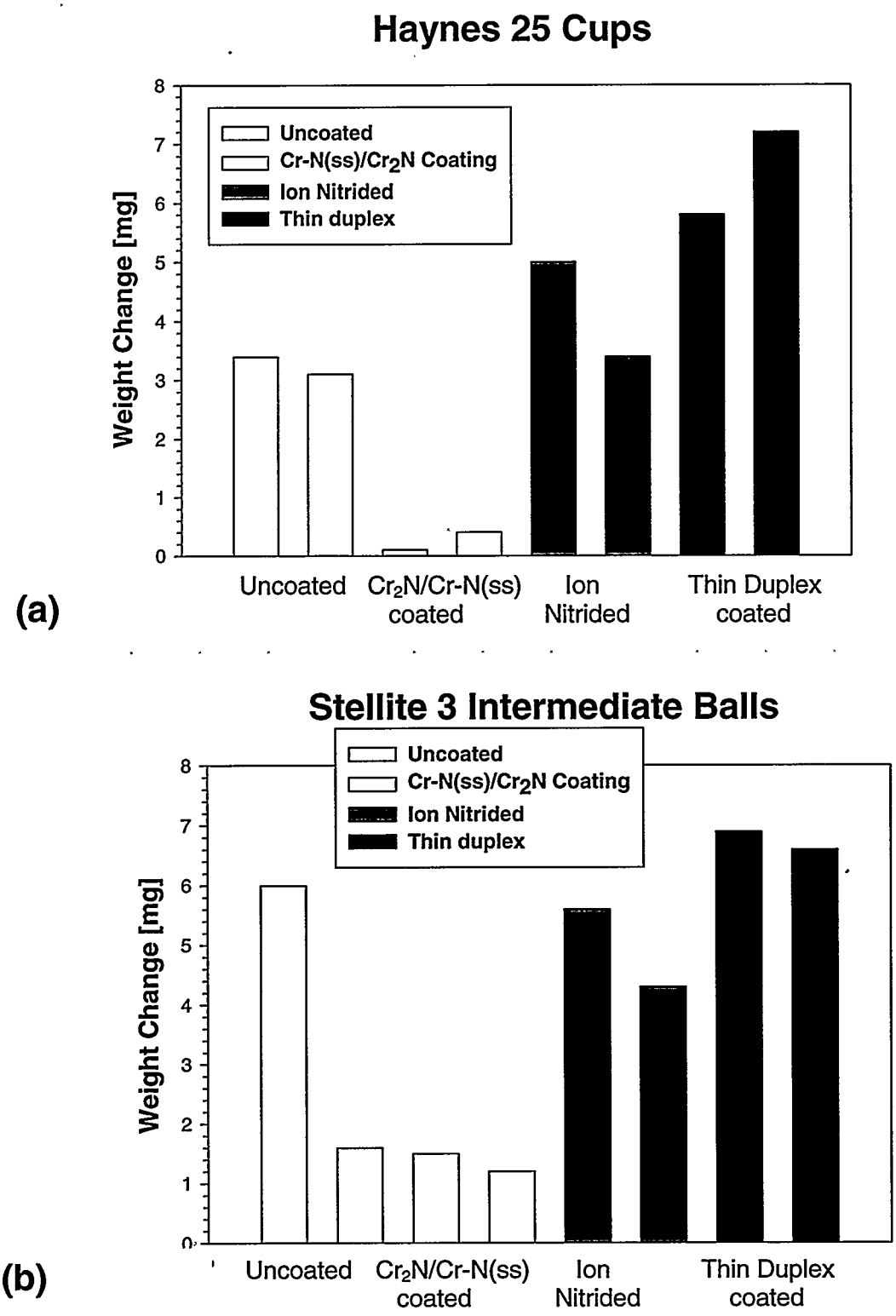

Figure 5. Plots of weight change for the uncoated, Cr_2N/Cr-N(ss) coated, ion nitrided, and thin duplex coated test specimens after 4-ball wear testing. Results are given for two tests at each condition with data grouped by test pieces: (a) Haynes 25 cups, (b) total weight change for all three Stellite 3 intermediate balls, (c) Haynes 25 drive ball, and (d) 17-4 PH separator, which was not coated in any of the tests.

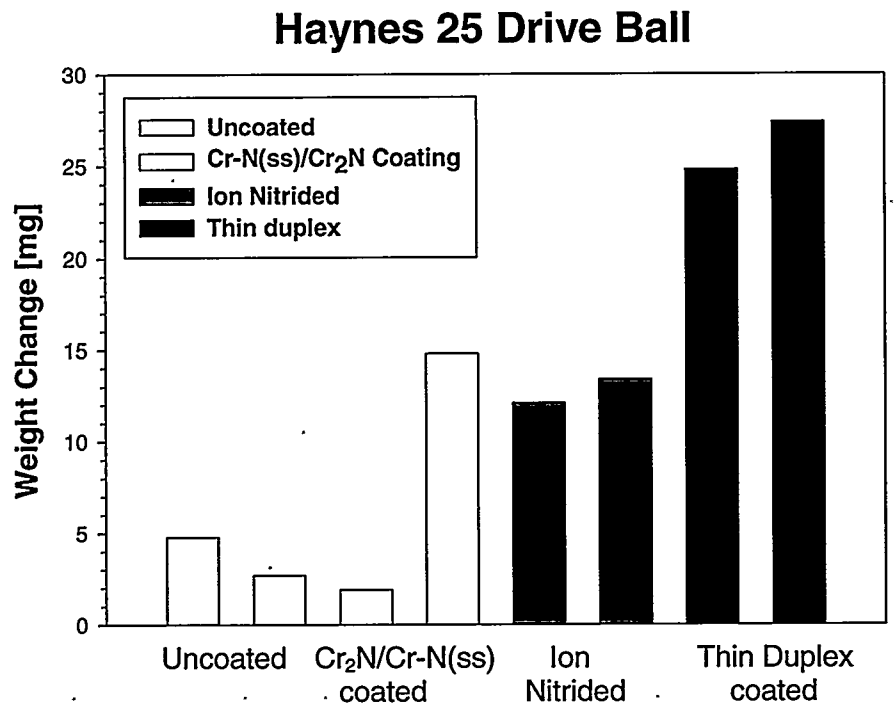

(c)

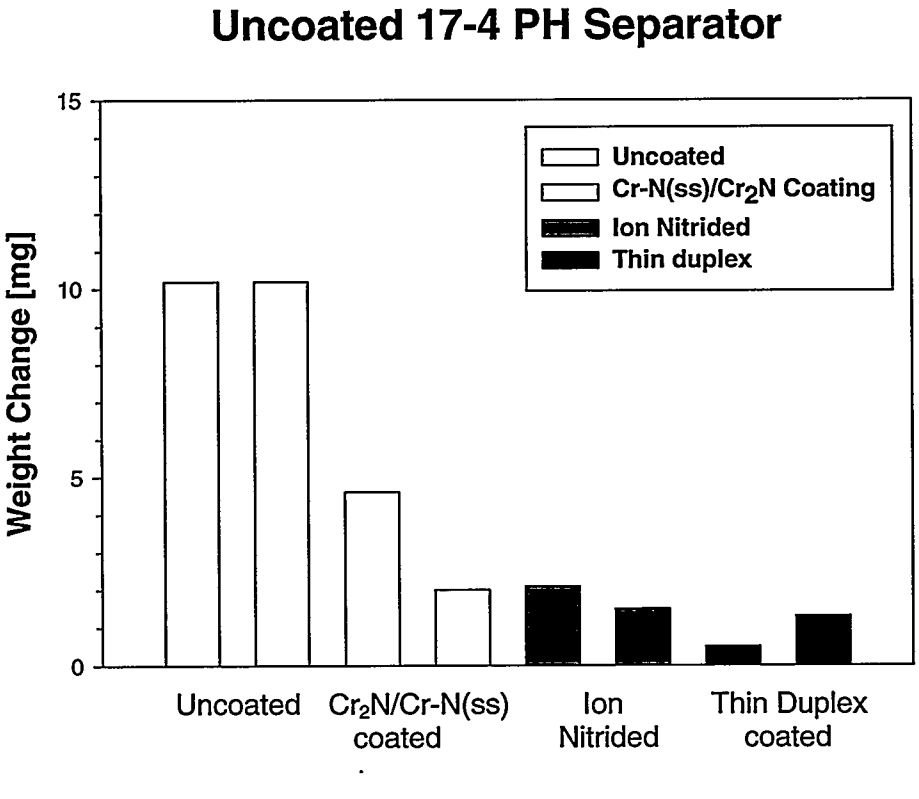

(d)

Figure 5. (Continued).

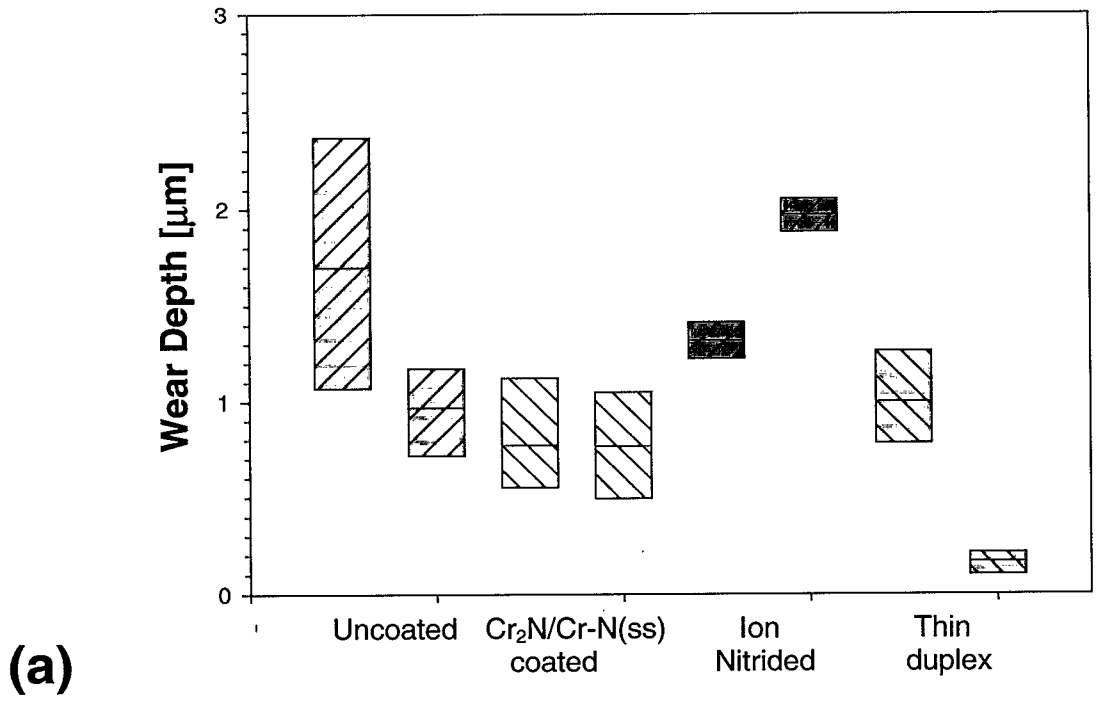

(a)

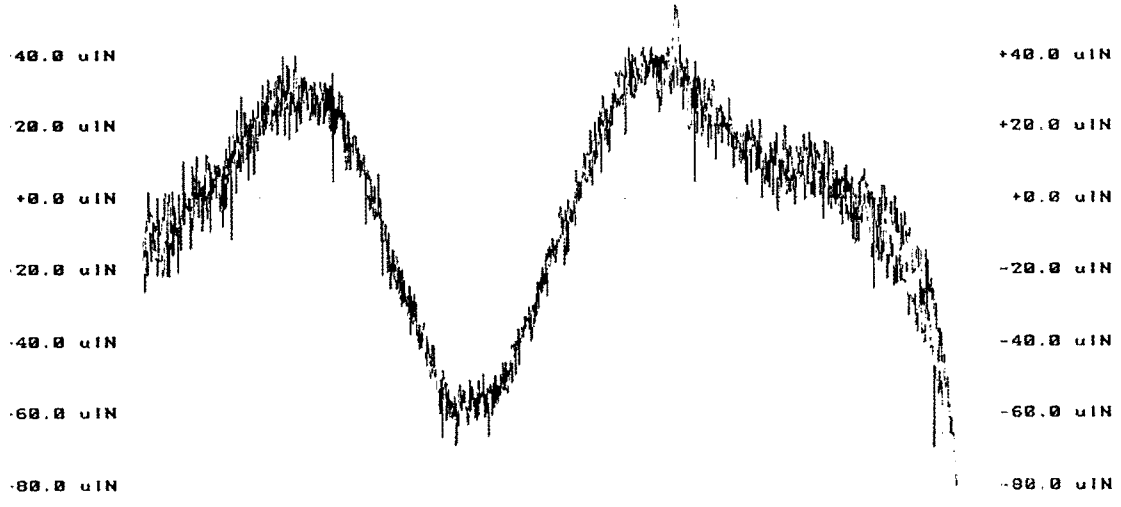

(b)

Figure 6. Post-test wear examinations of Haynes 25 cup specimens from 4-ball wear test: (a) range of wear depth measurements made using pre-test and post-test profilometry measurements, (b) pre-test and post-test profilometry measurements for the Cr_2N/Cr-N(ss) coated specimen, (c) pre- and post-test profilometry measurements of the uncoated specimen, (d) Cr_2N/Cr-N(ss) coated cup showing a rare region of minor coating damage, and (e) surface of a Cr_2N/Cr-N(ss) coated Stellite 3 intermediate ball showing one region of minor coating damage.

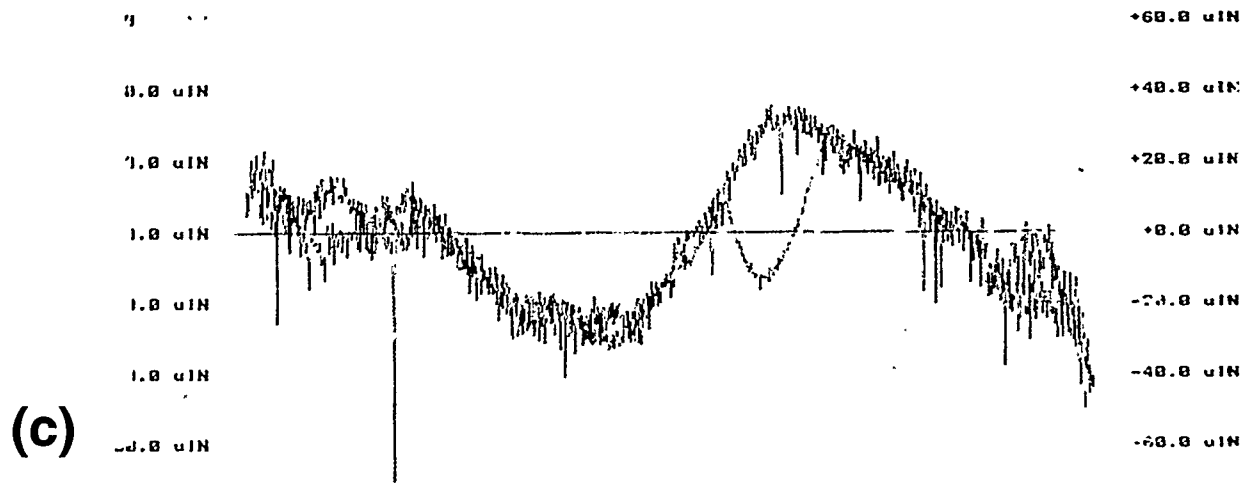

(c)

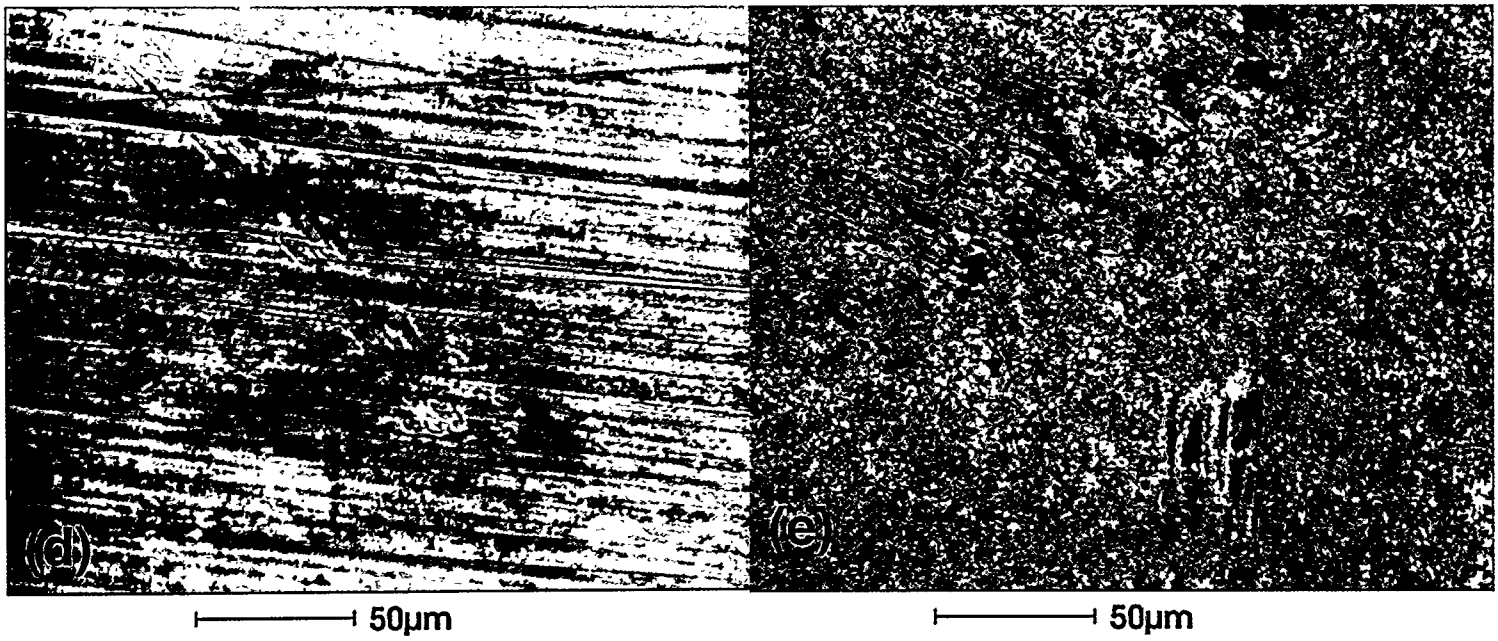

Figure 6. (Continued)

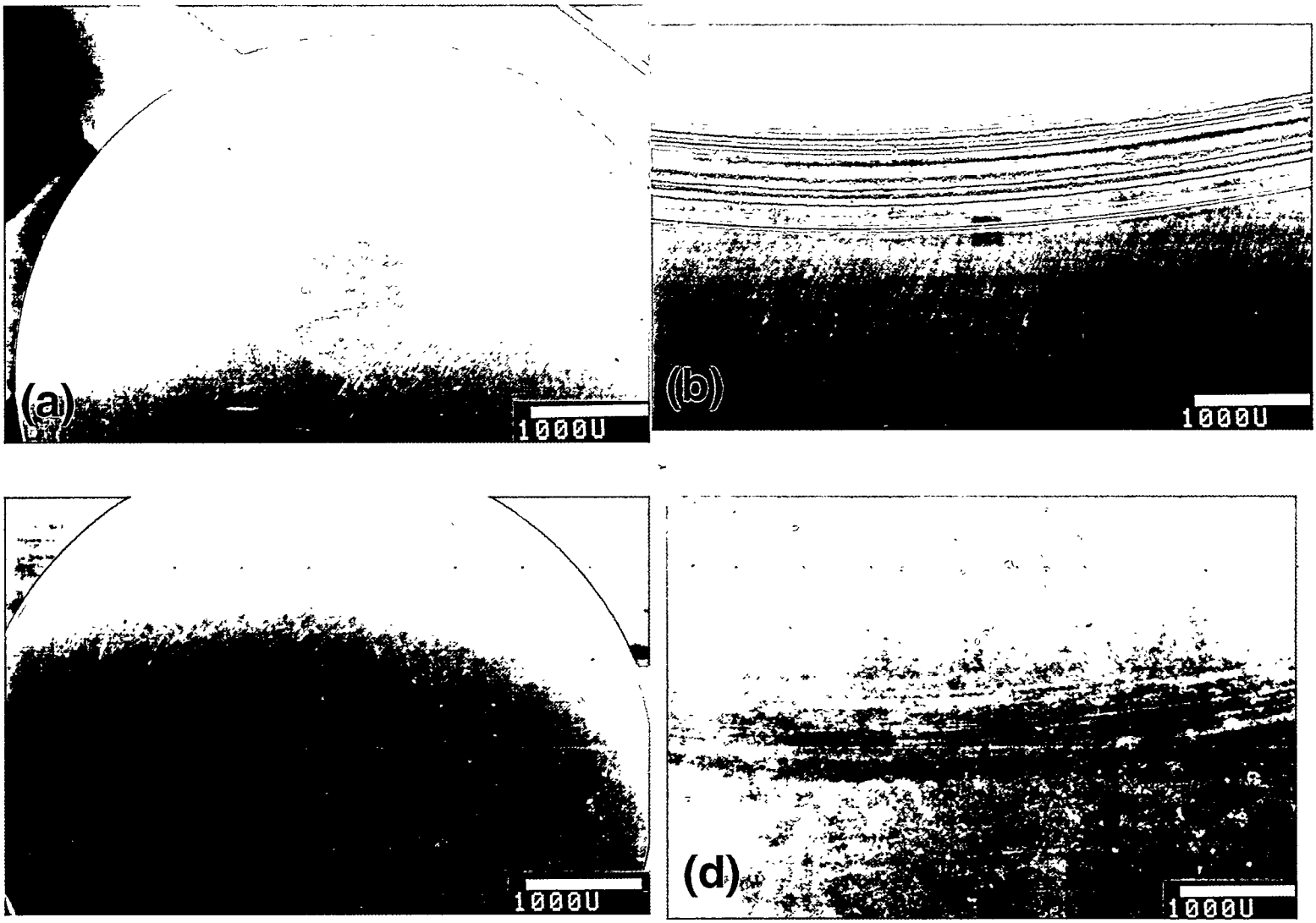

Figure 7. SEM examinations of the pin and disc coupons at low magnification (20X) after pin-on-disc testing: (a) uncoated Stellite 3 pin showing adhesively transferred wear debris, (b) uncoated Haynes 25 disc, (c) Cr_2N/Cr-N(ss) coated Stellite 3 pin showing the tip was worn flat, and (d) Cr_2N/Cr-N(ss) coated Haynes 25 disc.

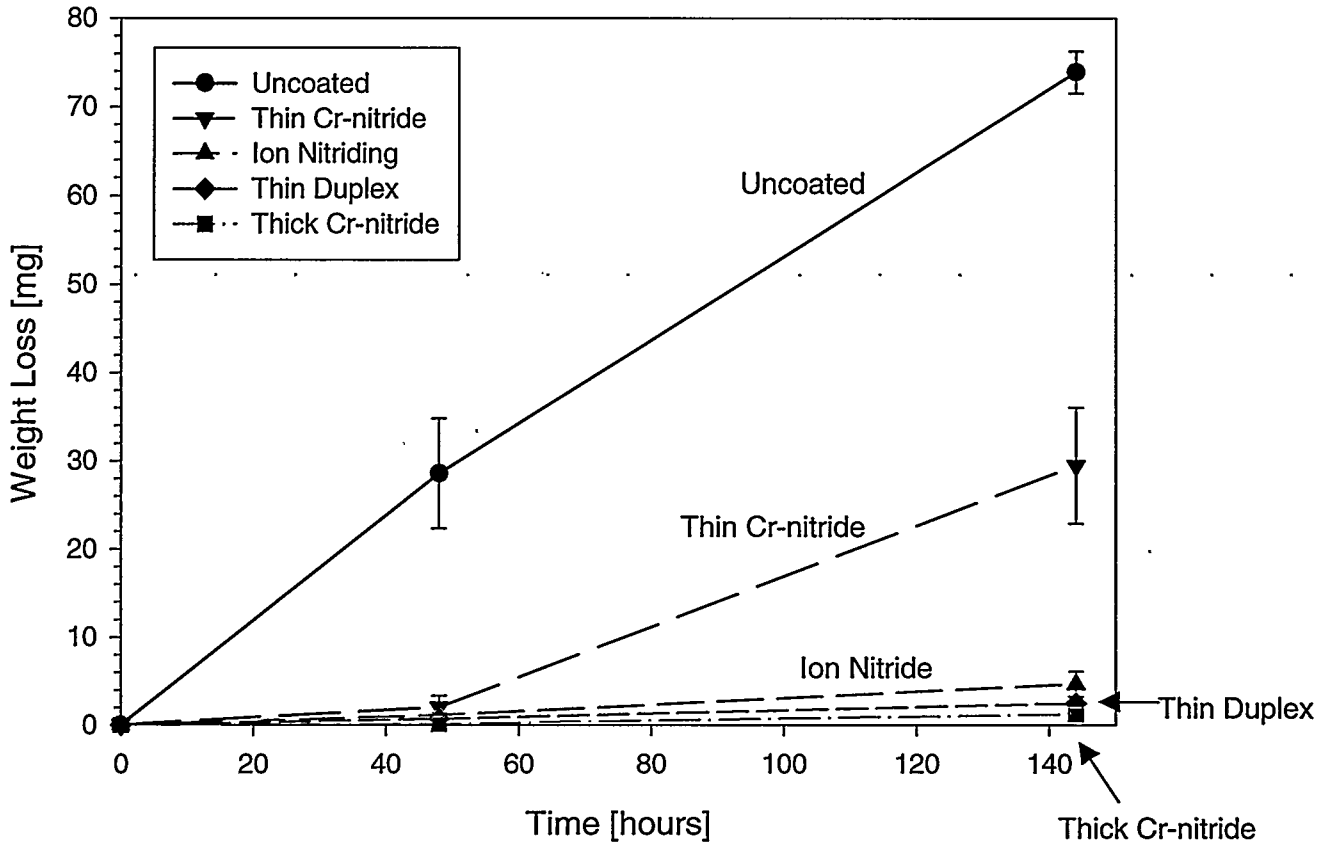

Figure 8. Haynes 25 roller average weight loss as a function of test time for the 48h and 144h (48h + 96h) RC test of uncoated and coated rollers. The weight change data were taken from Table 4. The error bars are one standard deviation.

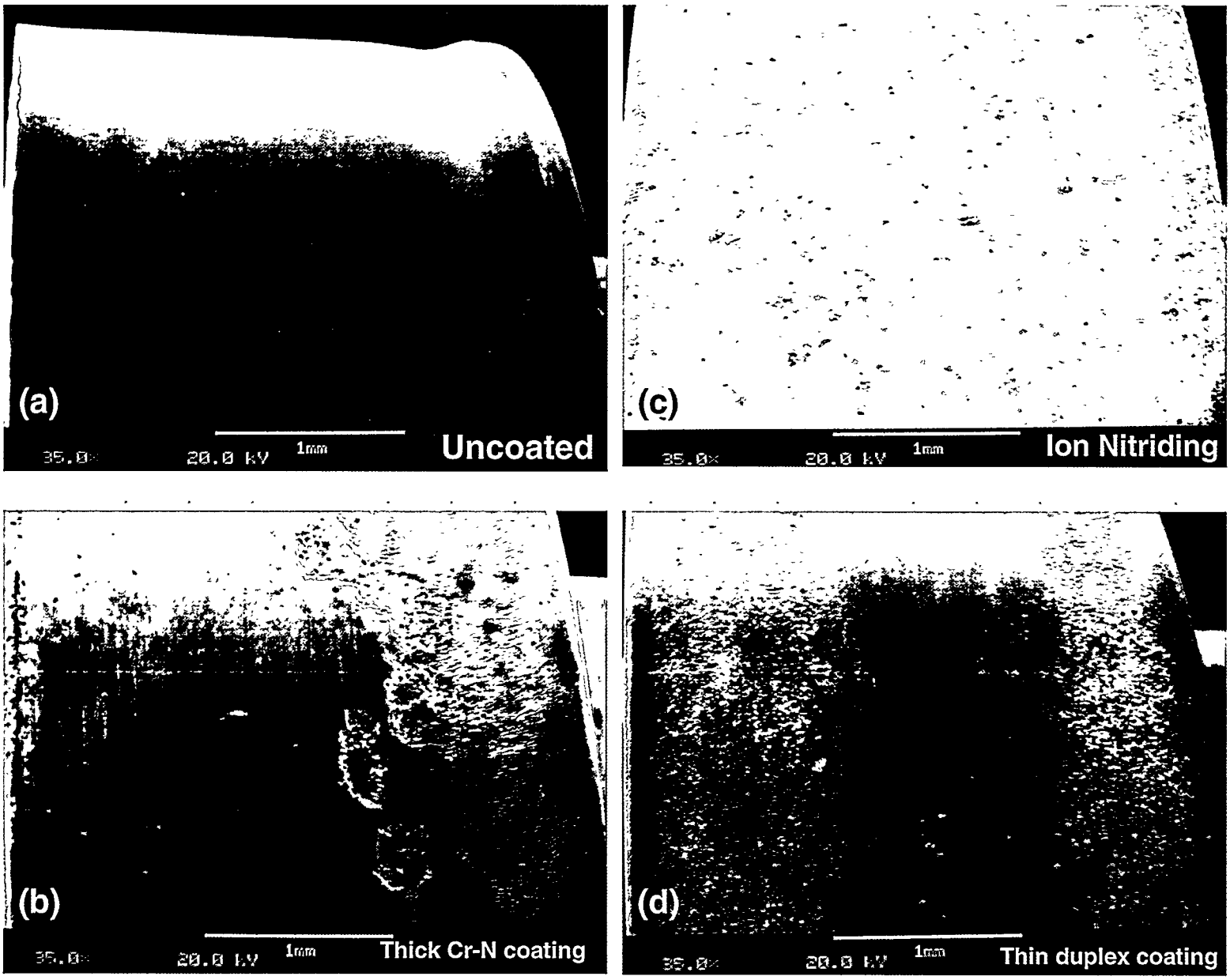

Figure 9. Low magnification (35X) SEM images of Haynes 25 rollers after the 144 hour (48h + 96h) phase of RC wear testing: (a) uncoated roller with unworn region on the right, (b) thick four-layer Cr_2N/Cr-N(ss)/Cr_2N/Cr-N(ss) coated roller, (c) ion nitrided roller, and (d) thin duplex coated roller.

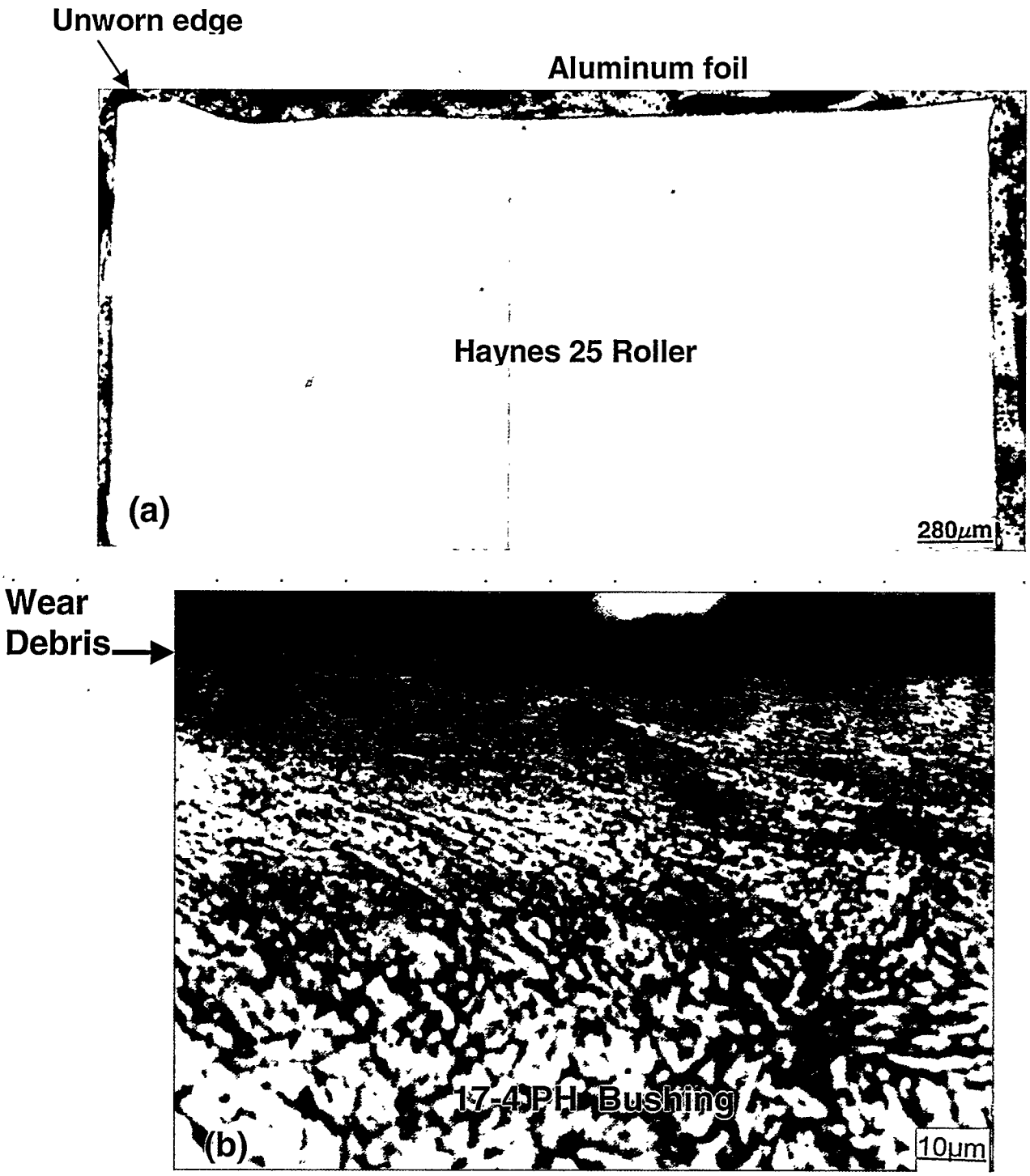

Figure 10. Metallographic sections of uncoated rollers and bushings after the 144h (48h + 96h) RC wear test: (a) uncoated roller with the unworn edge of the roller on the left (Mag=50X), and (b) wear surface of the bushing showing wear debris (Mag=1000X).

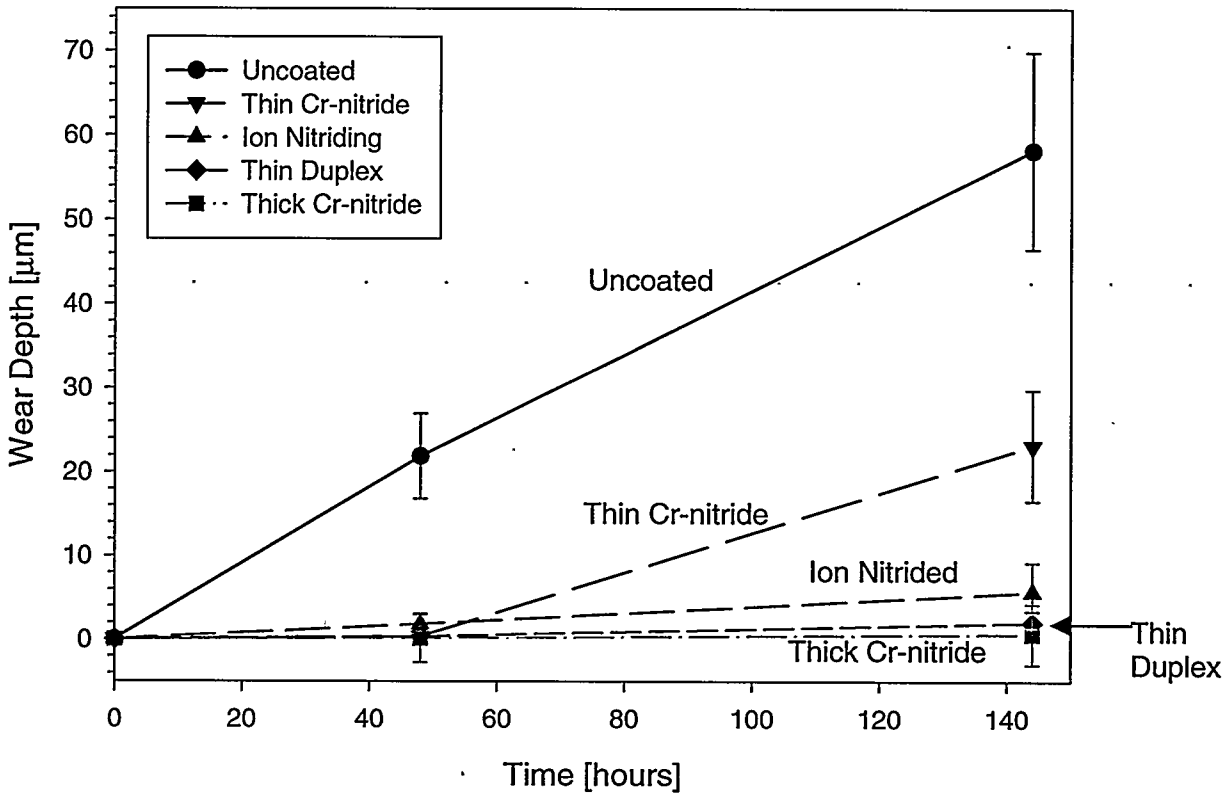

Figure 11. Summary plot of average wear depth measured from metallographic sections of the Haynes 25 rollers after the RC wear test. The measured data were taken from Table 5. The error bars are one standard deviation.

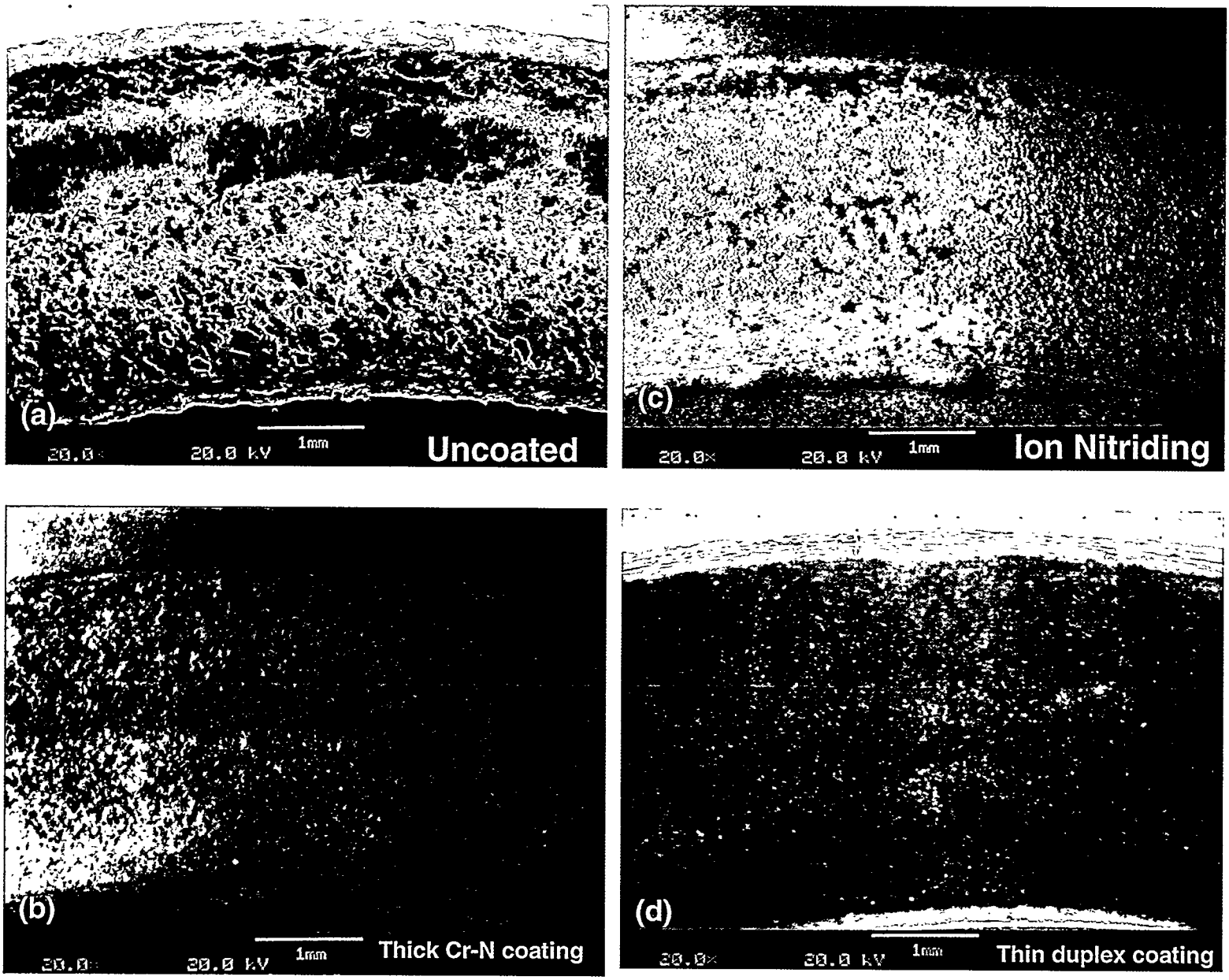

Figure 12. Low magnification (20X) SEM/BSE images of uncoated 17-4 PH bushings following the 144 hour (48h + 96h) phase of RC wear testing: (a) bushing mated with uncoated roller showing adherent wear debris on the outer edge of the bushing, (b) bushing that was mated with the thick four-layer Cr_2N/Cr-N(ss)/Cr_2N/Cr-N(ss) coated roller, (c) bushing that was mated with the ion nitrided roller, and (d) bushing that was mated with the thin duplex coated roller.

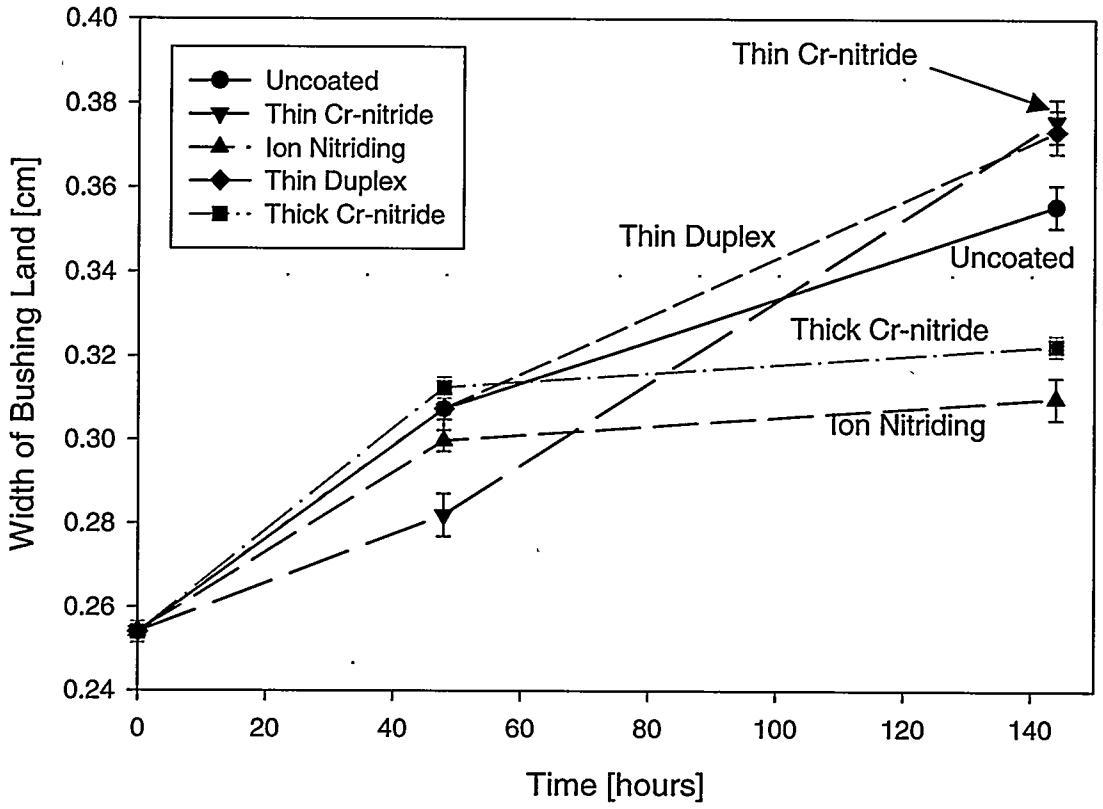

Figure 13. Average width of 17-4 PH bushing wear as a function of test time against uncoated and various coated Haynes 25 rollers in the Rolling Contact (RC) wear test. The measured data were taken from Table 6. The error bars are one standard deviation.

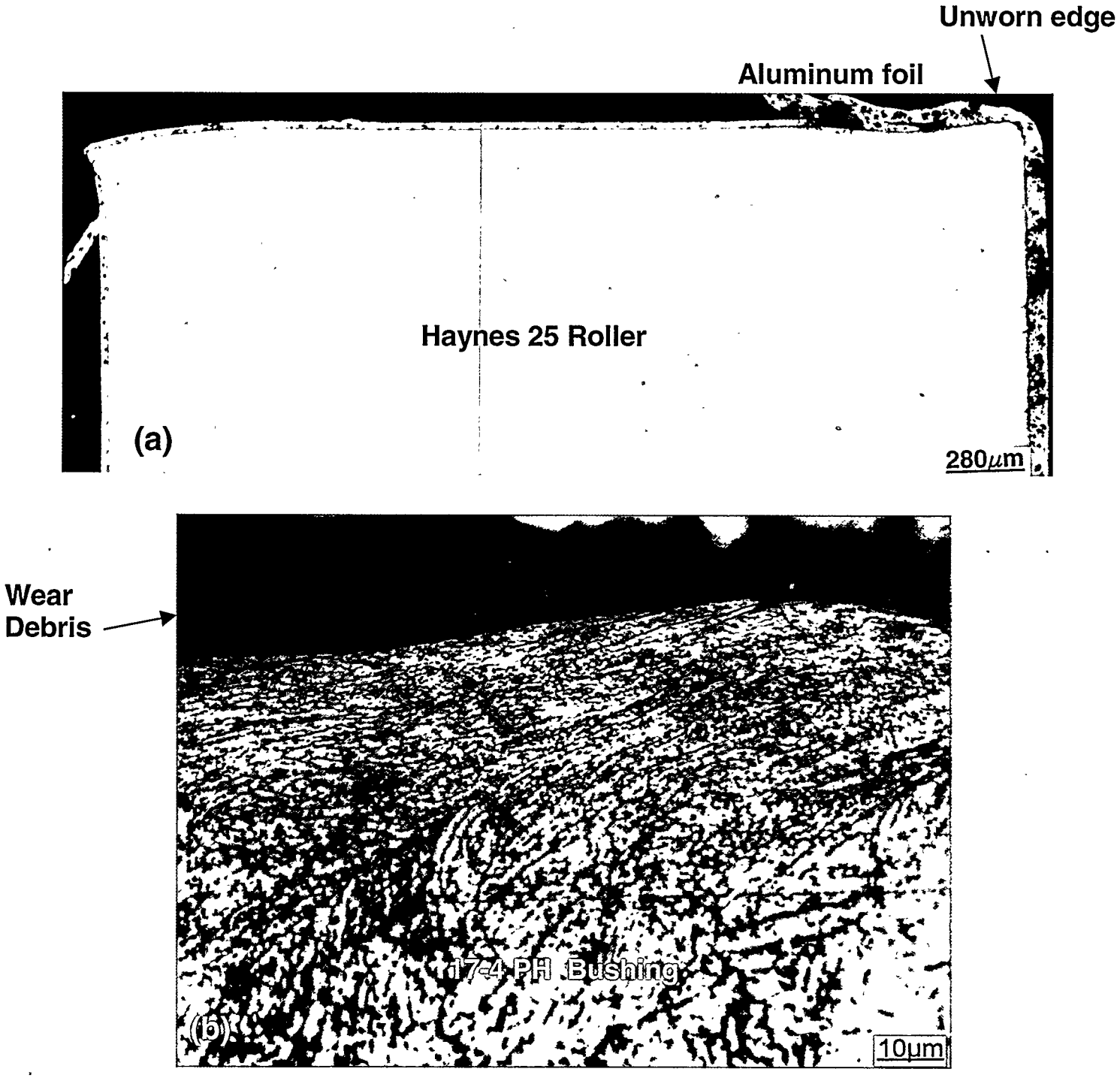

Figure 14. Metallographic cross-sections of thin dual-layer Cr_2N/Cr-N(ss) coated roller and mating bushing following the 144h (96h + 48h) phase of RC wear testing: (a) roller with the unworn edge on the right (Mag=50X), and (b) wear surface of the bushing (Mag=1,000X).

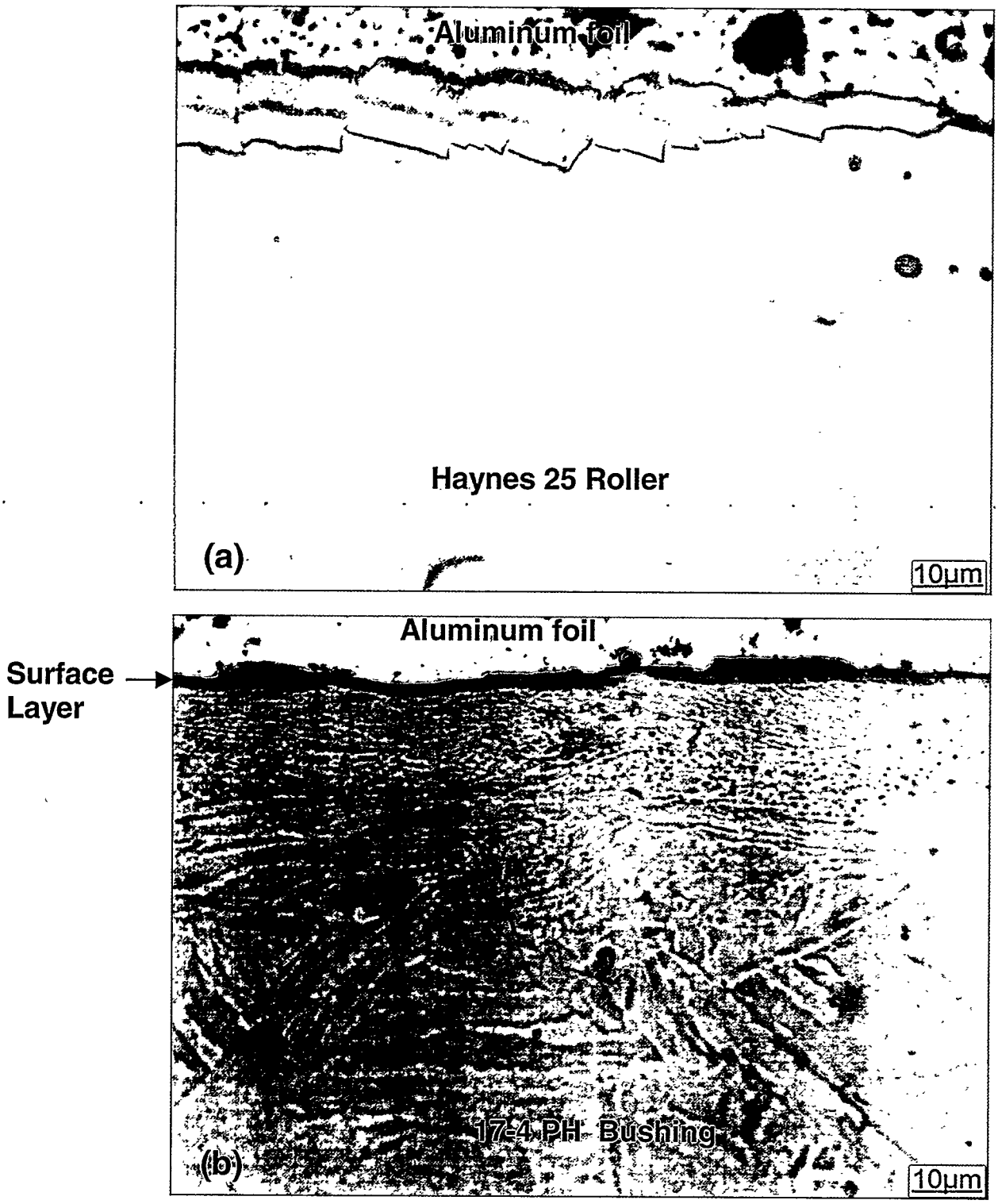

Figure 15. Metallographic cross-sections of the wear surface of the thick four-layer Cr_2N/Cr-N(ss)/Cr_2N/Cr-N(ss) coated roller and mating bushing after the 144h (96h + 48h) phase of RC wear testing: (a) roller surface showing coating damage and deadhesion on the right side (Mag=1,000X), and (b) wear surface of the bushing showing a thin surface layer (Mag=1,000X).

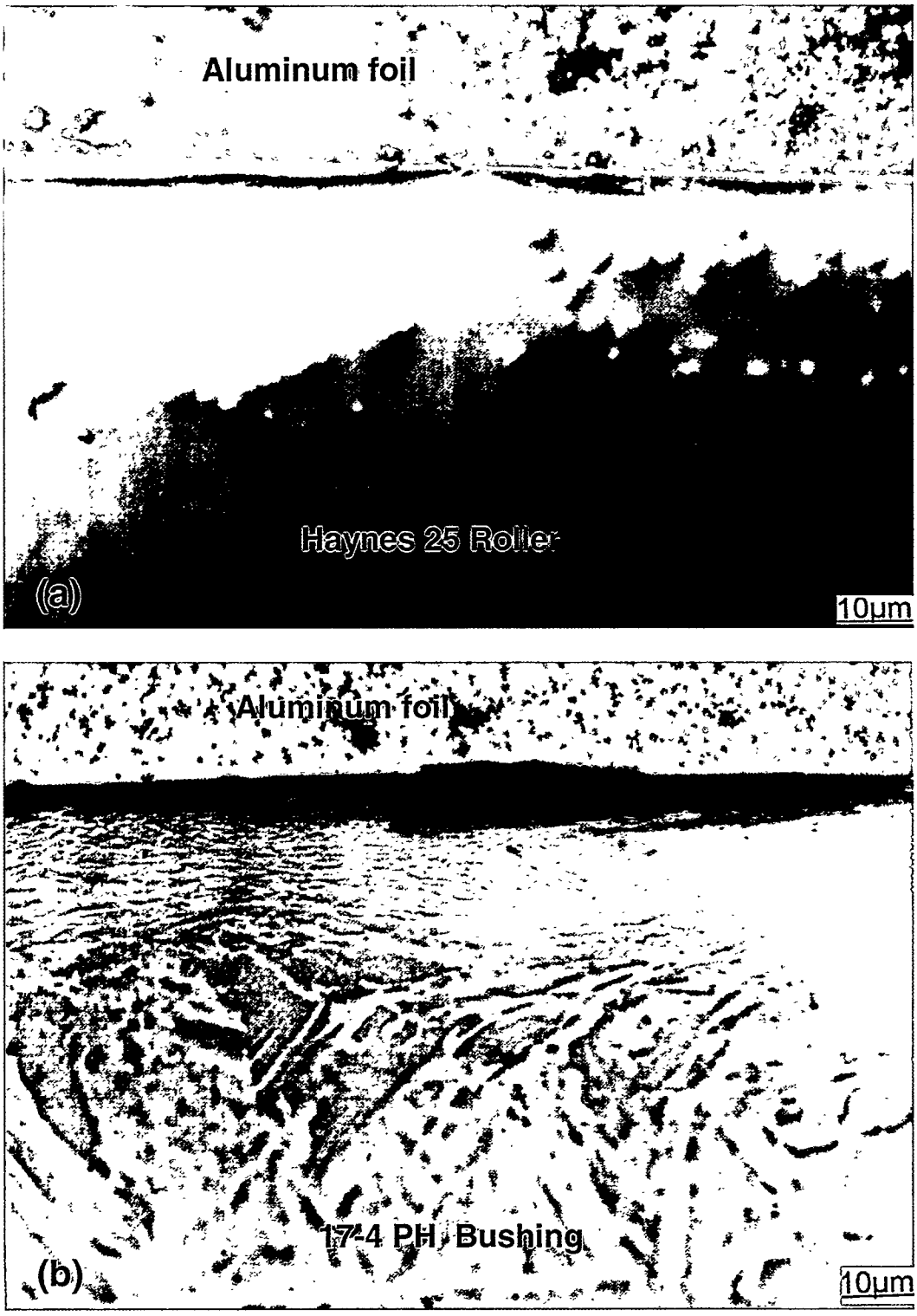

Figure 16. Metallographic cross-sections of the wear surface of the ion nitrided roller and mating bushing after the 144h (96h + 48h) phase of RC wear testing: (a) roller surface showing that the nitride layer has been worn very thin (Mag=1,000X), and (b) wear surface of the bushing showing with some wear debris (Mag=1,000X).

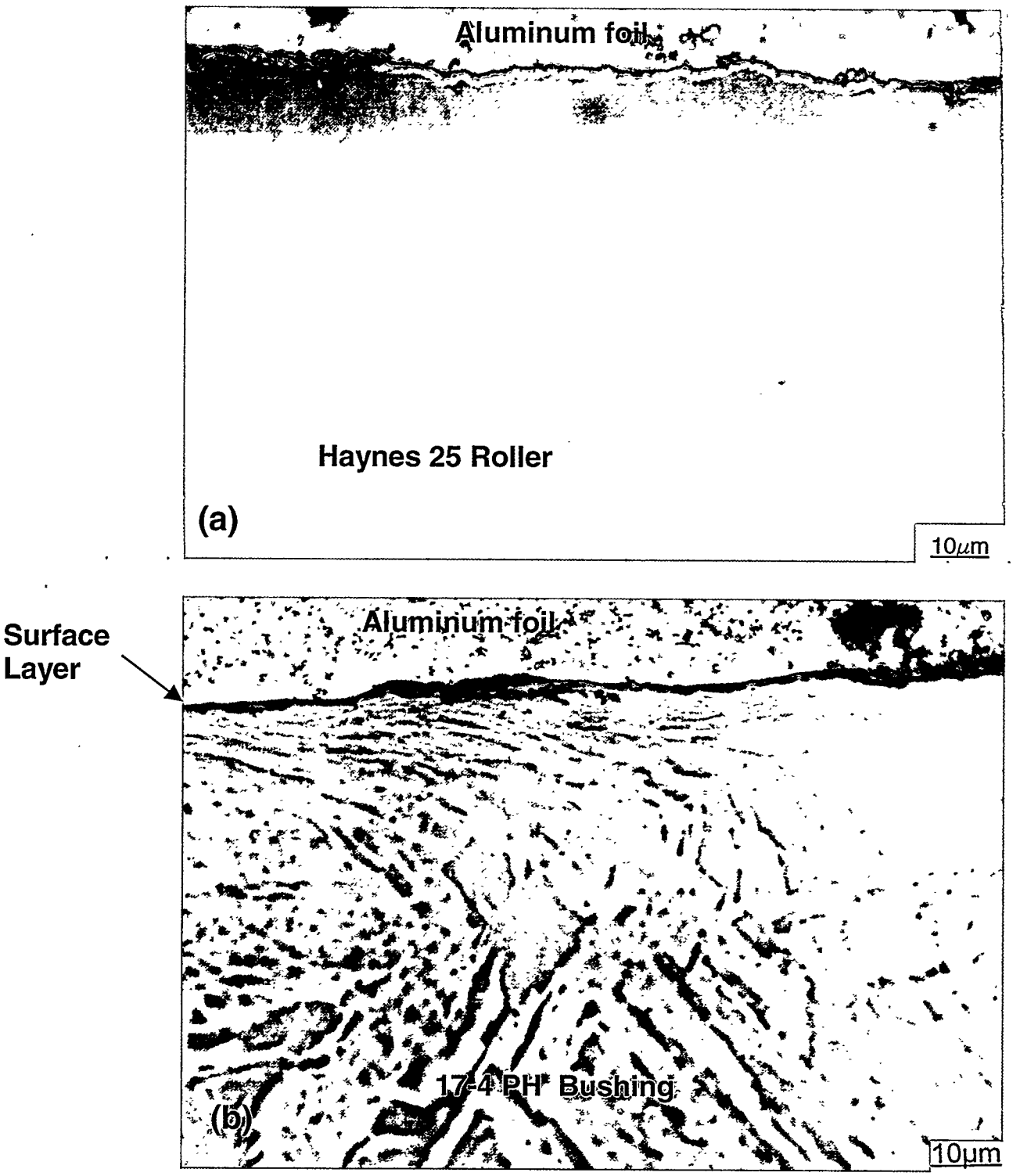

Figure 17. Metallographic cross-sections of the wear surface of the thin duplex coated roller and mating bushing following the 144h (96h + 48h) phase of RC wear testing: (a) roller surface showing the outer Cr_2N/Cr-N(ss) coating and nitride layer of the thin duplex coating (Mag=1,000X), and (b) wear surface of the bushing showing a thin surface layer (Mag=1,000X).

List of Figure captions.

Figure 1. Schematic drawings of the specimens used in the Rolling Contact (RC) wear test: (a) Haynes 25 roller, and (b) 17-4 PH bushing. All dimensions are in cm. Drawing not to scale.

Figure 2. Cross-sectional metallography of multilayer chromium-nitride coatings deposited on Haynes 25: (a) optical metallography of thin, dual-layer Cr_2N/Cr-N(ss) coating (Mag=1,000X) after etching showing the thin Cr_2N and Cr-N(ss) layers, (b) SEM/BSE micrograph of thick, four-layer Cr_2N/Cr-N(ss)/Cr_2N/Cr-N(ss) coating showing the Cr_2N and Cr-N(ss) layers (Mag=2,000X), (c) chromium X-ray map of Fig. 2b, and (d) nitrogen X-ray map of Fig. 2b.

Figure 3. Cross-sectional metallography of the nitride layer produced by ion nitriding at 566°C for 48 hours: (a) SEM/BSE micrograph of the nitride layer grown on Haynes (Mag=1,500X), (b) nitrogen X-ray map of Fig. 3a, (c) optical micrograph of etched cross-section showing the diffusion zone and nitride layer (Mag=500X), (d) optical micrograph of etched section showing the nitride layer grown on Stellite 3 (Mag=1,000X), and (e) SEM image of the surface of ion nitrided Haynes 25 showing the iron-rich surface nodules and a nano-scratch indentation.

Figure 4. Metallographic section of duplex coatings deposited on Haynes 25: (a) SEM/BSE image of thin duplex coating (Mag.=2,000X), (b) nitrogen X-ray map of Figure 4a with a line profile, (c) SEM/BSE image of thick duplex coating at 2,000X magnification, and (d) nitrogen X-ray map of Figure 4c with a nitrogen line profile.

Figure 5. Plots of weight change for the uncoated, Cr_2N/Cr-N(ss) coated, ion nitrided, and thin duplex coated test specimens after 4-ball wear testing. Results are given for two tests at each condition with data grouped by test pieces: (a) Haynes 25 cups, (b) total weight change for all three Stellite 3 intermediate balls, (c) Haynes 25 drive ball, and (d) 17-4 PH separator, which was not coated in any of the tests.

Figure 6. Post-test wear examinations of Haynes 25 cup specimens from 4-ball wear test: (a) range of wear depth measurements made using pre-test and post-test profilometry measurements, (b) pre-test and post-test profilometry measurements for the Cr_2N/Cr-N(ss) coated specimen, (c) pre- and post-test profilometry measurements of the uncoated specimen, (d) Cr_2N/Cr-N(ss) coated cup showing a rare region of minor coating damage, and (e) surface of a Cr_2N/Cr-N(ss) coated Stellite 3 intermediate ball showing one region of minor coating damage.

Figure 7. SEM examinations of the pin and disc coupons at low magnification (20X) after pin-on-disc testing: (a) uncoated Stellite 3 pin showing adhesively transferred wear debris, (b) uncoated Haynes 25 disc, (c) Cr_2N/Cr-N(ss) coated Stellite 3 pin showing the tip was worn flat, and (d) Cr_2N/Cr-N(ss) coated Haynes 25 disc.

Figure 8. Haynes 25 roller average weight loss as a function of test time for the 48h and 144h (48h + 96h) RC test of uncoated and coated rollers. The weight change data were taken from Table 4. The error bars are one standard deviation.

Figure 9. Low magnification (35X) SEM images of Haynes 25 rollers after the 144 hour (48h + 96h) phase of RC wear testing: (a) uncoated roller with unworn region on the right, (b) thick four-layer Cr_2N/Cr-N(ss)/Cr_2N/Cr-N(ss) coated roller, (c) ion nitrided roller, and (d) thin duplex coated roller.

Figure 10. Metallographic sections of uncoated rollers and bushings after the 144h (48h + 96h) RC wear test: (a) uncoated roller with the unworn edge of the roller on the left (Mag=50X), and (b) wear surface of the bushing showing wear debris (Mag=1000X).

Figure 11. Summary plot of average wear depth measured from metallographic sections of the Haynes 25 rollers after the RC wear test. The measured data were taken from Table 5. The error bars are one standard deviation.

Figure 12. Low magnification (20X) SEM/BSE images of uncoated 17-4 PH bushings following the 144 hour (48h + 96h) phase of RC wear testing: (a) bushing mated with uncoated roller showing adherent wear debris on the outer edge of the bushing, (b) bushing that was mated with the thick four-layer Cr_2N/Cr-N(ss)/Cr_2N/Cr-N(ss) coated roller, (c) bushing that was mated with the ion nitrided roller, and (d) bushing that was mated with the thin duplex coated roller.

Figure 13. Average width of 17-4 PH bushing wear as a function of test time against uncoated and various coated Haynes 25 rollers in the Rolling Contact (RC) wear test. The measured data were taken from Table 6. The error bars are one standard deviation.

Figure 14. Metallographic cross-sections of thin dual-layer Cr_2N/Cr-N(ss) coated roller and mating bushing following the 144h (96h + 48h) phase of RC wear testing: (a) roller with the unworn edge on the right (Mag=50X), and (b) wear surface of the bushing (Mag=1,000X).

Figure 15. Metallographic cross-sections of the wear surface of the thick four-layer Cr_2N/Cr-N(ss)/Cr_2N/Cr-N(ss) coated roller and mating bushing after the 144h (96h + 48h) phase of RC wear testing: (a) roller surface showing coating damage and deadhesion on the right side (Mag=1,000X), and (b) wear surface of the bushing showing a thin surface layer (Mag=1,000X).

Figure 16. Metallographic cross-sections of the wear surface of the ion nitrided roller and mating bushing after the 144h (96h + 48h) phase of RC wear testing: (a) roller surface showing that the nitride layer has been worn very thin (Mag=1,000X), and (b) wear surface of the bushing showing with some wear debris (Mag=1,000X).

Figure 17. Metallographic cross-sections of the wear surface of the thin duplex coated roller and mating bushing following the 144h (96h + 48h) phase of RC wear testing: (a) roller surface showing the outer Cr_2N/Cr-N(ss) coating and nitride layer of the thin duplex coating (Mag=1,000X), and (b) wear surface of the bushing showing a thin surface layer (Mag=1,000X).